NASA TECHNICAL MEMORANDUM

NASA TM X-64661

BOUNDARY LAYER LOSS SENSITIVITY STUDY USING A MODIFIED ICRPG TURBULENT BOUNDARY LAYER COMPUTER PROGRAM

by Satoaki Omori, Alfred Krebsbach, and Klaus W. Gross
Astronautics Laboratory

March 3, 1972

NASA

George C. Marshall Space Flight Center
Marshall Space Flight Center, Alabama

MSFC - Form 3190 (Rev June 1971)

TECHNICAL REPORT STANDARD TITLE PAGE

1. REPORT NO.	2. GOVERNMENT ACCESSION NO.	3. RECIPIENT'S CATALOG NO.
TM X 64661		

4. TITLE AND SUBTITLE	5. REPORT DATE
Boundary Layer Loss Sensitivity Study Using a Modified ICRPG Turbulent Boundary Layer Computer Program	March 3, 1972
	6. PERFORMING ORGANIZATION CODE
7. AUTHOR(S)	8. PERFORMING ORGANIZATION REPORT #
Satoaki Omori*, Alfred Krebsbach, and Klaus W. Gross	
9. PERFORMING ORGANIZATION NAME AND ADDRESS	10. WORK UNIT NO.
George C. Marshall Space Flight Center Marshall Space Flight Center, Alabama 35812	11. CONTRACT OR GRANT NO.
	13. TYPE OF REPORT & PERIOD COVERED
12. SPONSORING AGENCY NAME AND ADDRESS	Technical Memorandum
National Aeronautics and Space Administration Washington, D. C. 20546	14. SPONSORING AGENCY CODE

15. SUPPLEMENTARY NOTES

Prepared by Astronautics Laboratory, Science and Engineering
* National Research Council, National Academy of Sciences, Washington, D. C.

16. ABSTRACT

Modifications of the JANNAF Turbulent Boundary Layer (TBL) computer program refer to a more accurate representation of boundary layer edge conditions, internal calculation of the Prandtl number, a changed friction coefficient relationship, and computation of the performance degradation.

Significant differences in the results of the original and modified TBL programs are presented.

Important input parameters of the modified TBL program such as wall temperature distribution, Prandtl number, Stanton number, and velocity profile exponent were changed and the individual effects on significant boundary layer parameters, heat transfer, and performance degradation are described.

17. KEY WORDS	18. DISTRIBUTION STATEMENT
Turbulent boundary layers Rocket thrust chamber performance Nozzle flow Heat transfer	Klaus W. Gross Unclassified - Unlimited

19. SECURITY CLASSIF. (of this report)	20. SECURITY CLASSIF. (of this page)	21. NO. OF PAGES	22. PRICE
Unclassified	Unclassified	52	$3.00

MSFC - Form 3292 (May 1969)

TABLE OF CONTENTS

LIST OF ILLUSTRATIONS

LIST OF ILLUSTRATIONS (Concluded)

LIST OF TABLES

TECHNICAL MEMORANDUM X-64661

BOUNDARY LAYER LOSS SENSITIVITY STUDY USING A MODIFIED ICRPG TURBULENT BOUNDARY LAYER COMPUTER PROGRAM

SUMMARY

The original JANNAF Turbulent Boundary Layer computer program was modified to use accurate boundary layer edge conditions in the calculation process instead of the internally calculated properties based upon ideal gas relationships. The Prandtl number, assumed to be constant in the original model, is determined internally at each geometric station. Also the friction coefficient relationship has been slightly changed. Comparison of results from the original and modified programs indicates that the performance degration, the displacement thickness, and the temperature thickness are affected significantly.

A study investigating the effect of important input parameters of the modified TBL version on the heat transfer and the performance degradation provides the following results:

- A constant wall temperature or a wall temperature distribution shows a small effect on the heat transfer and performance degradation, if these temperature differences are moderate.

- Consideration of a constant or internally calculated Prandtl number affects the heat transfer considerably since this quantity is contained in the Stanton number equation. The boundary layer thickness parameters are only slightly affected.

- Use of two different Stanton number relationships produces a significant heat transfer variation and affects boundary layer thickness parameters considerably.

- Variation of the velocity profile exponent shows a definite effect on the boundary layer thicknesses and the performance degradation. The larger the exponent $1/n$, the larger is the influence on performance. The heat transfer is hardly affected by the velocity profile.

During this study a rocket thrust chamber using liquid oxygen and liquid hydrogen at a chamber pressure of P_c = 3000 psia (210.9 kgf/cm^2) and a mixture ratio of MR = 6.0, expanding the reaction products to an area ratio of ϵ = 57, was used as a reference case.

INTRODUCTION

In the original TBL program the boundary conditions of the boundary layer are represented by the wall temperature distribution along the chamber contour and by free stream flow properties correlated with a Mach number and geometry relationship along the boundary layer edge. Since the flow in the thrust chamber is chemically reactive during the expansion process, the edge conditions are not adequately determined from the ideal gas analogy. Therefore, the original program was modified to use profiles of Mach number, static pressure, static temperature, velocity, and mean molecular weight from an external source [JANNAF Two-Dimensional Kinetic (TDK) Computer Program] as boundary layer edge conditions. The specific heat ratio and the gas constant are internally calculated from a provided specific heat-temperature relationship and the mean molecular weight input. The original constant Prandtl number assumption was also replaced by an equation to determine this quantity at every local station internally. In addition the skin friction coefficient equation has been replaced by a modified Blasius relation to improve the solution accuracy and to avoid multiple solutions that were encountered at Reynolds numbers greater than $R_{e_\theta} = 10^4$ with the original formulation.

To identify solution differences, a rocket thrust chamber, originally considered for the Space Shuttle vehicle, was selected as a sample case. The results obtained with the original and modified TBL programs indicate significant differences and are presented in this document.

A performance degradation analysis with the TBL program depends to a great extent on the input data. Therefore, a parametric study was conducted to identify the sensitivity of performance degradation and heat transfer with regard to certain input parameters. The critical input parameters must be determined to a much higher degree of accuracy than the ones showing only a minor effect.

In this study the individual effects of the wall temperature distribution, Prandtl number, Stanton number, and the exponent of the velocity profile on the various boundary layer parameters, heat transfer, and performance degradation are determined with the modified TBL program. The results are documented and compared with the reference case.

The documentation of the original TBL program [1] was supplemented by an additional document [2] providing a detailed calculation sequence, a specific description of each subroutine, and derivations of the important equations used in the TBL program.

The modified TBL computer program called TBL-I is available at S&E-ASTN-PPB, NASA, Marshall Space Flight Center.

MODIFICATION OF THE JANNAF TBL COMPUTER PROGRAM

The original TBL computer program [1] provided by the JANNAF Liquid Rocket Performance Committee internally computes the velocity, pressure, density, and temperature in the free stream of the combustion products from an ideal gas relationship. The reaction products flowing in the nozzle at a high temperature still react chemically even in the divergent section of the nozzle and are not accurately represented by the ideal gas analogy. Therefore, the TBL program was modified to accept tables of static pressure, static temperature, velocity, and mean molecular weight in addition to the thrust chamber contour and Mach number tables. These table values can be obtained from the JANNAF ODK or TDK programs [3, 4] or from another external source.

Density (ρ_∞)

The density of the combustion products ρ_∞ is calculated from the perfect gas relation at each axial location,

$$\rho_\infty = \frac{P_\infty \mathfrak{M}}{\mathcal{R} T_\infty} \quad , \tag{1}$$

where $\mathcal{R}$, P_∞, T_∞, and $\mathfrak{M}$ are the universal gas constant, static pressure, static temperature, and the mean molecular weight of the combustion products specified by the input tables. The subscript ∞ signifies the free stream condition. Equation (1) indicates that the density is affected by the mean molecular weight and that the specific gas constant represented by the ratio of the universal gas constant and the molecular weight is changing throughout the thrust chamber.

Specific Heat Ratio (γ_∞)

The specific heat ratio γ_∞ can be represented by a speed of sound or Mach number relationship,

$$\gamma_\infty = \frac{\mathfrak{M} U_\infty^2}{M_\infty^2 \mathcal{R} T_\infty} \quad , \tag{2}$$

or by thermodynamic properties,

$$\gamma_\infty = \frac{C_{p\infty}}{C_{p\infty} - \frac{\mathcal{R}}{\mathfrak{M}}} \quad , \tag{3}$$

where M_∞ , U_∞ , and $C_{p\infty}$ denote the Mach number, velocity, and specific heat at constant pressure, respectively, at each location within the thrust chamber.

Combining equations (2) and (3) provides an expression for the specific heat $C_{p\infty}$,

$$C_{p\infty} = \frac{\frac{\mathcal{R}}{\mathfrak{M}} U_\infty^2}{U_\infty^2 - \frac{M_\infty^2 \mathcal{R} T_\infty}{\mathfrak{M}}} \quad . \tag{4}$$

This equation could replace the existing specific heat-temperature input table in the program. However, since the C_p-T input table is equivalent to the previous relationship and to avoid extensive reprogramming, the input table option was retained.

Another option exists to calculate the mean molecular weight $\mathfrak{M}$ at each local station from an input table identifying the specific heat $C_{p\infty}$ at each axial station,

$$\mathfrak{M} = \mathcal{R}\left(\frac{1}{C_{p\infty}} + \frac{M_\infty^2 T_\infty}{U_\infty^2}\right) \quad . \tag{5}$$

The modified TBL program calculates the specific heat ratio γ_∞ from equation (3) using the mean molecular weight table input. The specific heat at constant pressure $C_{p\infty}$ is provided by the table input relationship $C_{p\infty} = f(T_\infty)$ as in the original TBL program.

Prandtl Number (P_r)

The Prandtl number appears in the empirical relation of the Stanton number and by definition represents a quantity based upon laminar flow. When the flow passes through the throat section, considerable changes occur in the Prandtl number. Therefore, the constant Prandtl number assumption has been replaced by an internal calculation of this parameter. Based upon the definition of the laminar Prandtl number,

$$P_r = \frac{\mu_\infty C_{p\infty}}{\lambda_\infty} \quad , \tag{6}$$

where μ_∞ and λ_∞ represent the viscosity and the thermal conductivity of the combustion products, the following equation was derived (Appendix A) and incorporated into the program:

$$P_r = \frac{\gamma_\infty}{\frac{9}{4}\gamma_\infty - \frac{5}{4}} \quad . \tag{7}$$

This relation clearly shows the influence of the specific heat ratio γ_∞ which in turn depends on the mean molecular weight $\mathfrak{M}$ and the specific heat according to equation (3). A typical curve of Prandtl number variation for a nozzle flow field will be shown later in Figure 3.

Skin Friction Coefficient (C_f)

During operation of the original TBL program, multiple solutions of the skin friction coefficient were encountered for a given Reynolds number R_{e_θ} (Appendix C). To avoid future calculation difficulties, Cole's skin

friction coefficient relationship was replaced by a modified Blasius correlation,

$$C_f\left(R_{e_\theta}\right) = \frac{0.025}{\left(R_{e_\theta}\right)^{0.25}} \quad , \tag{8}$$

where the Reynolds number uses the momentum thickness as the characteristic parameter,

$$R_{e_\theta} = \frac{\rho_\infty U_\infty \theta}{\mu_\infty} \quad . \tag{9}$$

According to experimental data [5], the constant in the previous equation should be 0.018 instead of 0.025, but to remain conservative the constant value of 0.025 was retained. In Figure 1 the curves representing the three discussed relationships are shown. The modified Blasius equation yields slightly higher values for the skin friction coefficient than Cole's relationship and is single valued in the higher Reynolds number range. Use of the constant 0.018 shifts the modified Blasius equation results to lower values.

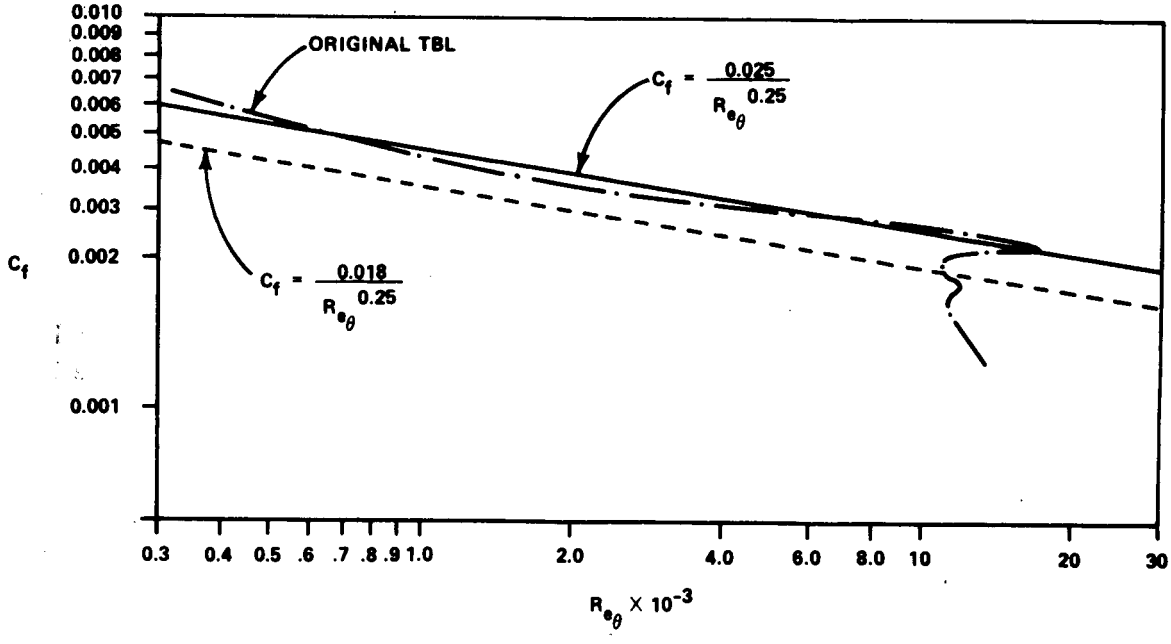

Figure 1. Skin-friction coefficient as a function of Reynolds number.

The skin friction coefficient $C_f\left(R_{e_\phi}\right)$ used in the Stanton number equation is replaced by a similar relationship,

$$C_f\left(R_{e_\phi}\right) = \frac{0.025}{\left(R_{e_\phi}\right)^{0.25}} \quad , \tag{10}$$

where the Reynolds number uses the energy thickness as the characteristic parameter,

$$R_{e_\phi} = \frac{\rho_\infty U_\infty \phi}{\mu_\infty} \quad . \tag{11}$$

Boundary Layer Performance Degradation

In a rocket nozzle performance prediction, the losses associated with the existence of a boundary layer are significant. The original TBL program provides only the necessary parameters to determine the thrust degradation. For convenience, this equation has been included in this program. Since performance and performance losses are quite commonly expressed in terms of specific impulse, approximate equations for the thrust chamber vacuum and sea level thrust were incorporated into the program. This modification provides the capability to determine the specific impulse and impulse loss caused by the boundary layer.

Two possibilities exist to determine the thrust degradation; these are dependent on the nozzle contour given.

1. If the real nozzle contour is given, it can be postulated that the inviscid flow field will be almost the same as the one obtained with the real contour corrected by the displacement thickness, because the latter value is small compared to the contour radii. In this case the total thrust produced by a one-dimensional inviscid flow can be calculated,

$$F_{vacuum} = \left[\pi\left(r - \delta^* \cos\alpha\right)^2 \left(P_\infty + \rho_\infty U_\infty{}^2\right)\right]_{exit} \quad . \tag{12}$$

and

$$F_{\text{sea level}} = \left[\pi\left(r - \delta^* \cos\alpha^2\right)\left(P_\infty - P_a + \rho_\infty U_\infty{}^2\right)\right]_{\text{exit}} . \quad (13)$$

The corresponding mass flow rate is

$$\dot{m} = \left[\rho_\infty U_\infty \pi(r - \delta^* \cos\alpha)^2\right]_{\text{exit}} . \quad (14)$$

In these equations r represents the real nozzle radius.

If the postulation of negligible flow field differences does not hold true because of a sizable boundary layer displacement thickness, an iteration on the inviscid flow field contour is necessary.

2. If the inviscid flow field contour is given, the thrust produced by a one-dimensional flow field is,

$$F_{\text{vacuum}} = \left[\pi r^2\left(P_\infty + \rho_\infty U_\infty{}^2\right)\right]_{\text{exit}} \quad (15)$$

and

$$F_{\text{sea level}} = \left[\pi r^2\left(P_\infty - P_a + \rho_\infty U_\infty{}^2\right)\right]_{\text{exit}} . \quad (16)$$

The corresponding mass flow rate is,

$$\dot{m} = \left[\rho_\infty U_\infty \pi r^2\right]_{\text{exit}} . \quad (17)$$

In these equations r represents the inviscid flow contour radius.

The specific impulse for the one-dimensional inviscid flow can now be calculated,

$$I_{sp_{\text{vacuum}}} = \frac{F_{\text{vacuum}}}{\dot{m}} \quad (18)$$

and

$$I_{sp_{\text{sea level}}} = \frac{F_{\text{sea level}}}{\dot{m}} \quad . \tag{19}$$

To calculate the thrust more accurately, the $\rho_\infty U_\infty$ at the nozzle exit can be obtained from a given mass flow rate $\dot{m}$. Depending on the real or inviscid flow contour, the mass flow density is

$$\rho_\infty U_\infty = \frac{\dot{m}}{\pi(r - \delta^* \cos\alpha)^2} \quad (r \equiv \text{real contour}) \tag{20}$$

and

$$\rho_\infty U_\infty = \frac{\dot{m}}{\pi r^2} \quad (r \equiv \text{inviscid contour}) \quad . \tag{21}$$

Multiplication of $\rho_\infty U_\infty$ by the boundary layer edge quantity U_∞ provides a more accurate result than the one obtained from the one-dimensional model.

The thrust degradation caused by the boundary layer effects can be determined from the following equation, as documented in Reference 2;

$$\Delta F_{B.L.} = \left\{ \left[2\pi r \, \rho_\infty U_\infty^2 \, \theta \cos\alpha \right] \left(1 - \frac{\delta^*}{\theta} \frac{P_\infty}{\rho_\infty U_\infty^2} \right) \right\}_{\text{exit}} , \tag{22}$$

where the displacement thickness δ^* and the momentum thickness θ are the only boundary layer parameters. All other terms represent quantities of the boundary layer edge at the nozzle exit.

The corresponding specific impulse loss is

$$\Delta I_{sp} = \frac{\Delta F_{B.L.}}{\dot{m}} \quad . \tag{23}$$

The modified TBL program contains equations (12), (13), (14), (18), (19), (22), and (23) since the real contour of the engine, used in the parameter study, was available.

COMPARISON OF RESULTS FROM THE ORIGINAL AND MODIFIED TBL COMPUTER PROGRAMS

A former Space Shuttle engine design was used as a sample case (Fig. 2) to show the difference in the boundary layer solutions obtained from the original and modified TBL programs. The original TBL program internally calculates the pressure P_∞, temperature T_∞, and velocity U_∞ in the free stream, whereas table values (Fig. 3 and Table 1) for these quantities and in addition the mean molecular weight $\mathfrak{M}$ along the boundary layer edge were used in the modified program. Because of difficulties encountered with the original skin friction coefficient calculation, the modified Blasius relationship was applied in both programs. A comparison of the results, shown in Table 2, indicates that the modified program calculates a specific impulse loss approximately 50 percent lower, a total heat transfer approximately 5 percent higher, a boundary layer displacement thickness approximately 100 percent higher, and a momentum thickness

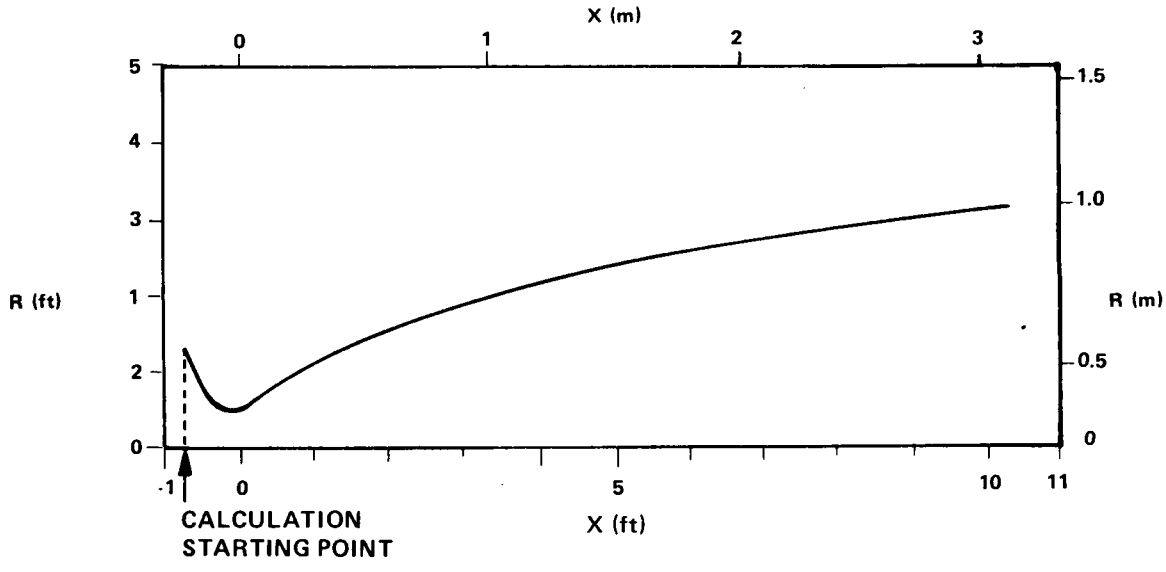

Figure 2. Thrust chamber nozzle contour.

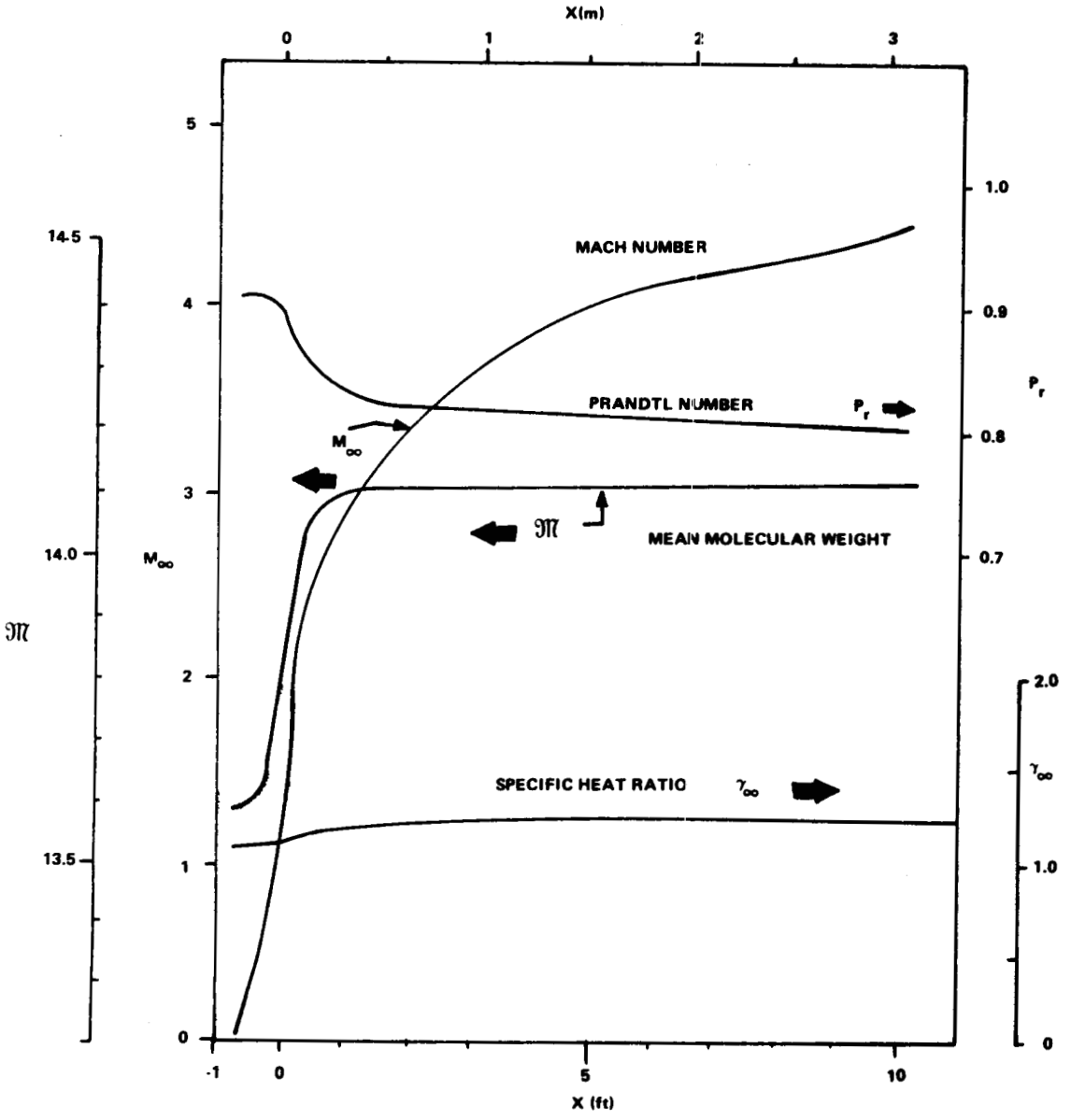

Figure 3. Inviscid nozzle flow properties as a function of nozzle length (reference case).

approximately 25 percent smaller as compared to the original TBL solution. All other solutions indicated only a slight deviation. The vacuum thrust calculation results differ significantly because of the internally calculated and tabular input nozzle exit parameters for the boundary layer edge. This comparison clearly indicates that considerable differences result in the performance degradation, heat transfer, and boundary layer parameters when the modified program is used.

TABLE 1. INPUT TABLES FOR MODIFIED TBL PROGRAM (REFERENCE CASE)

x (ft)	y (ft)	Mach Number	Pressure (lbf/ft^2)	Static Temperature (° R)	Velocity (ft/sec)	Molecular Weight (lbm/lbm mole)	Wall Temperature (° R)
- 0.74000000	1.28300001	0.06540000	430938.589844	6514.171265	341.998299	13.596038	1500.000000
- 0.70000000	1.24500000	0.08680000	430803.386719	6513.945374	449.713486	13.596115	1501.000000
- 0.65000000	1.15400000	0.11500000	430376.687500	6513.232483	601.322884	13.596359	1503.000000
- 0.60000000	1.04400000	0.14800000	429571.242187	6511.884766	773.783501	13.596819	1504.000000
- 0.55000000	0.93800000	0.18000000	428257.367187	6509.682068	940.903488	13.597570	1505.000000
- 0.50000000	0.84000000	0.21900000	426143.968750	6506.125793	1144.403244	13.598783	1507.000000
- 0.45000000	0.74800000	0.26000000	422584.132812	6500.097595	1357.922546	13.600837	1510.000000
- 0.40000000	0.67000000	0.30500000	417121.234375	6490.756226	1591.619995	13.604016	1512.000000
- 0.35000000	0.60000000	0.35500000	408201.140625	6475.257080	1849.983658	13.609287	1515.000000
- 0.30000000	0.54000000	0.42000000	394000.000000	6449.924011	2183.766510	13.617876	1517.000000
- 0.25000000	0.49300000	0.51000000	373266.746094	6411.375977	2642.587006	13.630889	1522.000000
- 0.20000000	0.46200000	0.67500000	348635.917969	6362.908875	3482.375977	13.647145	1525.000000
- 0.15000000	0.44200000	0.83900000	320962.054687	6304.489929	4305.792297	13.666566	1528.000000
- 0.10000000	0.43000000	0.91900000	290185.675781	6233.701660	4686.352600	13.689814	1530.000000
- 0.05000000	0.42500000	0.96900000	257635.841797	6150.690002	4904.364929	13.716626	1535.000000
0.00000000	0.42475000	1.00000000	248237.302734	6124.870544	5049.435852	13.724856	1540.000000
0.26667000	0.60067000	2.02399999	55255.762695	5103.002380	9304.507935	13.986906	1532.000000
0.70833000	0.94975000	2.70800000	14754.472656	4211.245239	11400.469604	14.087843	1504.000000
1.35833000	1.20132999	3.03000000	7766.364746	3790.732147	12161.423950	14.103885	1450.000000
1.67500000	1.34317000	3.18200001	5748.760010	3600.483795	12473.540039	14.107473	1415.000000
1.95833001	1.47142000	3.31400001	4502.654846	3449.974152	12737.706665	14.109281	1390.000000
2.54166999	1.69900000	3.51100001	3068.752136	3221.707977	13073.595337	14.110858	1310.000000
3.12500000	1.89950000	3.66999999	2282.654144	3052.450104	13327.146729	14.111449	1243.000000
3.91666999	2.12375000	3.83100000	1699.312439	2889.791168	13561.844360	14.111748	1163.000000
4.66666996	2.32642001	3.96599999	1336.023575	2761.740875	13746.858032	14.111872	1093.000000
6.58333004	2.68632999	4.18000001	914.612267	2568.120361	14007.482422	14.111960	951.000000
8.95833004	3.00342000	4.34299999	681.880005	2424.785431	14171.263184	14.111985	820.000000
10.19166994	3.20675001	4.44400001	573.919670	2343.315613	14273.130005	14.111992	780.000000

TABLE 2. COMPARISON OF SOLUTIONS OBTAINED FROM THE ORIGINAL AND MODIFIED TBL PROGRAMS (REFERENCE CASE)

	Modified TBL	Original TBL
F_{vacuum}, ton (lbf)	207.658 (457 810)	186.603 (411 390)
ΔF, ton (lbf)	-1.587 (-3499)	-2.072 (-4567)
ΔI_{sp}, sec	-3.53	-5.33
$\dot{q}_{w\ max}$, kcal/cm^2 sec (Btu/in.^{2} sec)	2.802 (71.7)	2.505 (64.1)
Q_w, kcal/sec (Btu/sec)	2.2574×10^4 (89 521)	2.1505×10^4 (85 622)
At nozzle exit		
δ^*, cm (ft)	1.92 (0.063)	0.88 (0.029)
δ, cm (ft)	6.00 (0.197)	6.98 (0.229)
Δ, cm (ft)	9.14 (0.300)	9.33 (0.306)
θ, cm (ft)	0.46 (0.015)	0.61 (0.020)
δ^*/θ	4.150	1.448
ϕ, cm (ft)	0.76 (0.025)	0.88 (0.029)
P_∞, T_∞, U_∞	Input	Internally calculated

Sonic Point Start

The original TBL program has the option of a sonic point start; i.e., the computation of the boundary layer can be started at the nozzle throat. This option, however, is limited to the adiabatic wall case. Furthermore, the assumptions are made that the temperature and velocity thicknesses are equal and the derivative of the momentum thickness is zero at the throat location.

Results from the modified TBL program indicate that the temperature and velocity thicknesses in the throat area are not equal (Figs. 4 and 5). The solutions of the original TBL program utilizing the sonic start point option and the ones obtained from the modified program starting the calculation in the chamber show remarkable differences as indicated in Table 3.

EFFECT OF SIGNIFICANT PARAMETERS ON PERFORMANCE AND HEAT TRANSFER

In the following paragraphs, the effect of some significant parameters on the performance degradation and heat transfer is discussed. The modified TBL program was used for this investigation. Parameters such as the wall temperature distribution, the Prandtl number, the Stanton number, and the velocity profile exponent were changed one at a time, and the results were compared with the reference case. The program input data for the reference case were obtained from Reference 6 and represent one-dimensional equilibrium solutions for a former Space Shuttle engine design (Figs. 2 and 3 and Tables 1, 4, and 5).

Effect of Wall Temperature Distribution

The reference case uses a wall temperature distribution as shown in Figure 6 and Table 1. This distribution was established using Reference 7 for the throat and Reference 8 for the divergent nozzle sections. Discontinuities at the end points were eliminated by plotting the individual temperature distributions and selecting points to obtain a smooth transition. To investigate the wall temperature sensitivity on performance degradation and heat transfer, this temperature profile was replaced by a constant temperature of $T_w = 1600°R$ (889°K) along the wall. The results of the TBL solutions are shown in Table 6 together with the reference case. Surprisingly the wall temperature variation has only a small effect on the performance degradation and heat transfer (approximately 4 percent lower for the constant wall temperature case).

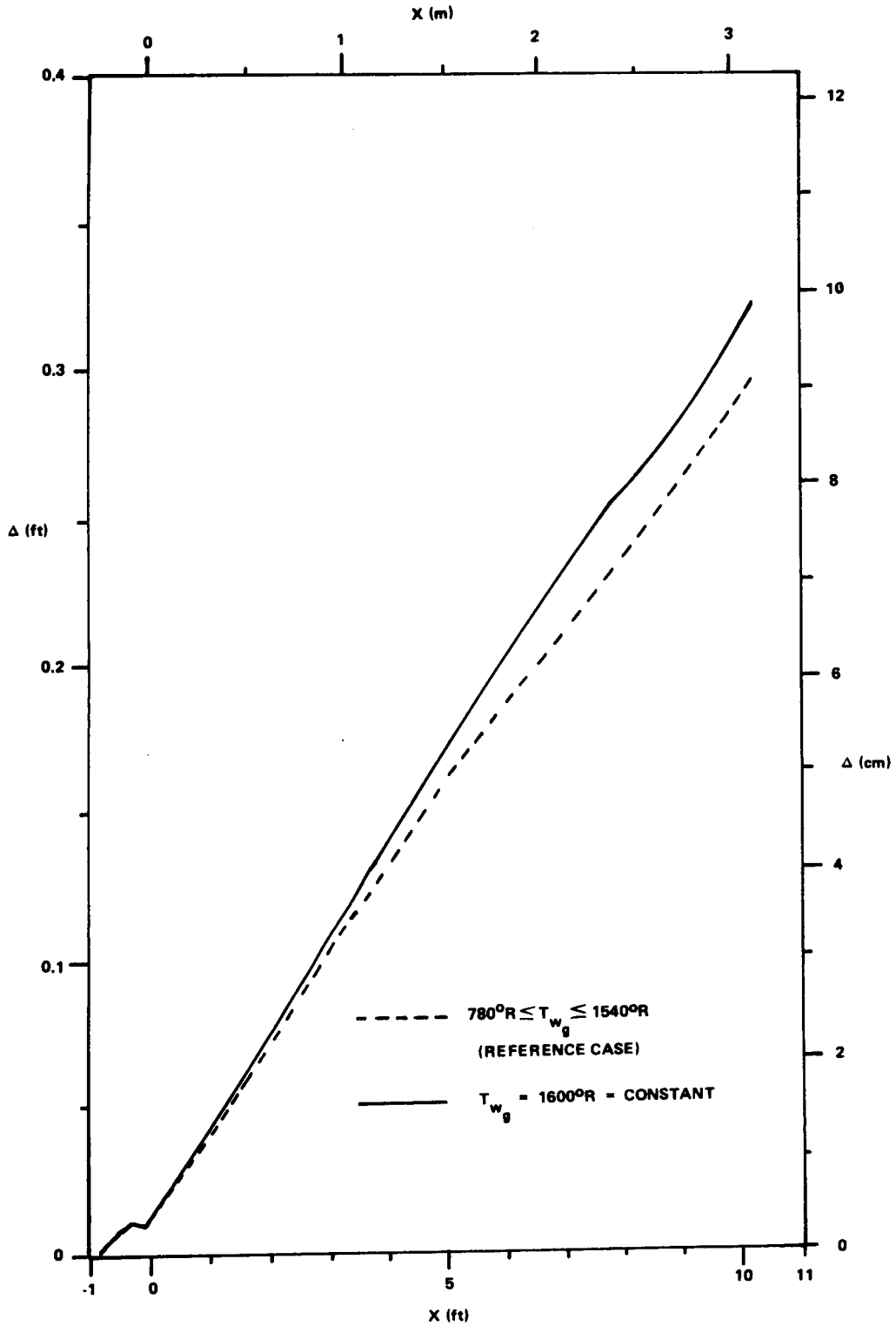

Figure 4. Effect of wall temperature on the temperature thickness.

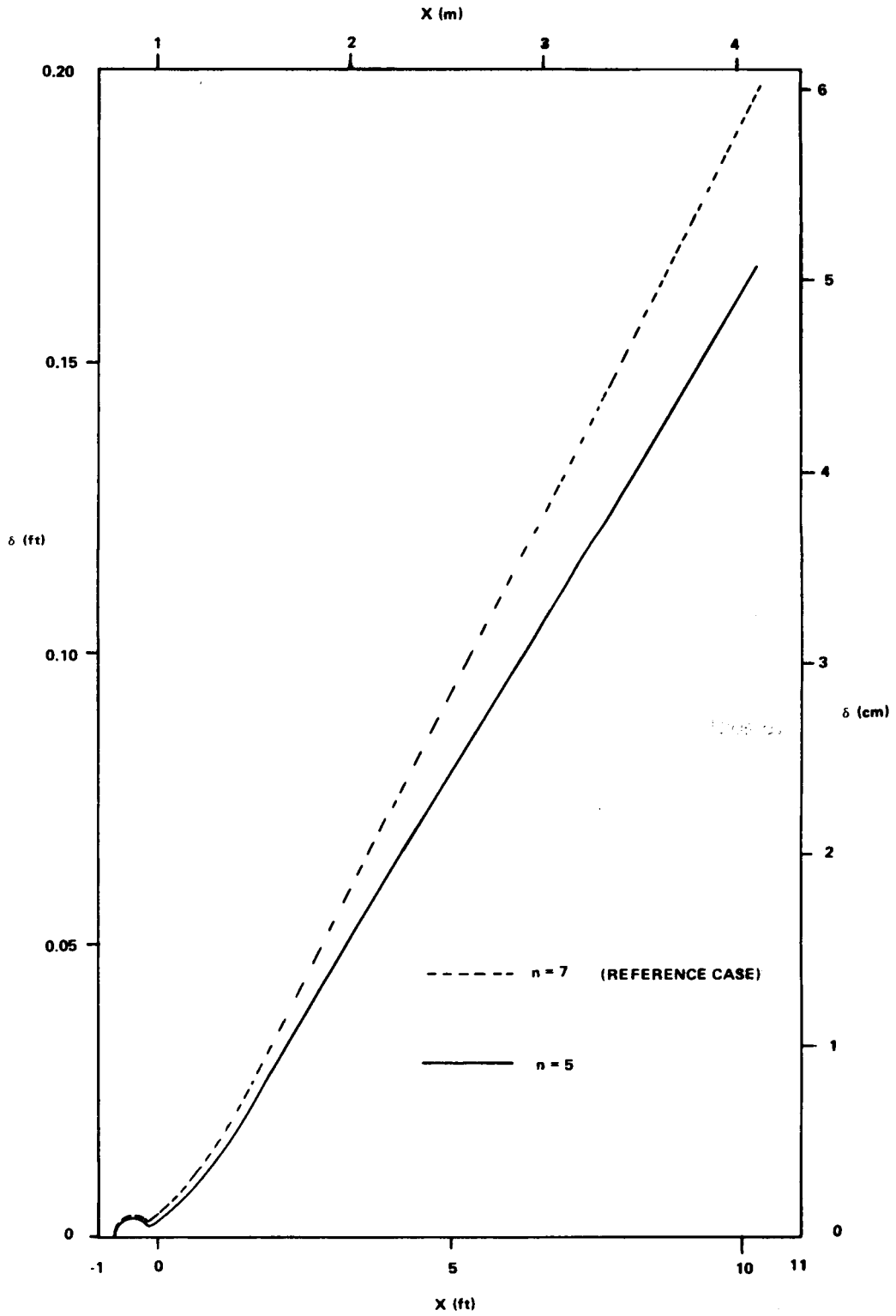

Figure 5. Effect of velocity profile power law on the velocity thickness.

TABLE 3. COMPARISON OF SOLUTIONS OBTAINED FROM THE MODIFIED TBL PROGRAM (REFERENCE CASE) AND THE ORIGINAL TBL PROGRAM SONIC START OPTION

	Modified TBL	Original Sonic Point Start
F_{vacuum}, ton (lbf)	207.658 (457 810)	202.337 (446 076)
ΔF, ton (lbf)	-1.587 (-3499)	-0.978 (-2157)
ΔI_{sp}, sec	-3.53	-2.23
$\dot{q}_{w\ max}$, kcal/cm^2 sec (Btu/in.^{2} sec)	2.802 (71.7)	0 (0.0)
Q_w, kcal/sec (Btu/sec)	2.2574×10^4 (89 521)	0 (0)
At nozzle exit		
δ^*, cm (ft)	1.92 (0.063)	3.17 (0.104)
δ, cm (ft)	6.00 (0.197)	7.07 (0.232)
Δ, cm (ft)	9.14 (0.300)	0.82 (0.027)
θ, cm (ft)	0.46 (0.015)	0.37 (0.012)
δ^*/θ	4.150	8.592
ϕ, cm (ft)	0.76 (0.025)	0.024 (0.0008)
P_r	Variable value	$P_r = 0.90$ = Constant
P_∞, T_∞, $\bar{U}_\infty$	Input	Internally calculated

TABLE 4. INPUT DATA FOR MODIFIED TBL PROGRAM (REFERENCE CASE)

MZETA	=	VELOCITY PROFILE POWER LAW EXPONENT	=	7
IPRINT	=	PRINT AT EVERY CALCULATED POINT (=1) OR AT INPUT INTERVALS (=0)	=	0
IXTAB	=	NUMBER OF POINTS IN X .VS. Y .VS. M TABLES	=	28
ICTAB	=	NUMBER OF POINTS IN CP .VS. T TABLE	=	20
ITWTAB	=	WALL TEMP. OPTION -- ADIABATIC (=-1), CONSTANT (=0), TABLE (=1)	=	1
T0	=	FREE STREAM STAGNATION TEMPERATURE	=	6.4978000+03
P0	=	FREE STREAM STAGNATION PRESSURE	=	4.3200000+05
GAM0	=	STAGNATION RATIO OF SPECIFIC HEATS	=	1.1490000+00
ZMU0	=	STAGNATION VISCOSITY	=	5.9330000-05
ZMVIS	=	EXPONENT OF VISCOSITY-TEMPERATURE LAW	=	7.5000000-01
ZNSTAN	=	BOUNDARY LAYER INTERACTION EXPONENT	=	1.0000000-01
DXMAX	=	MAXIMUM STEP SIZE	=	1.0931670-01
THETAI	=	INITIAL VALUE OF MOMENTUM THICKNESS	=	1.0000000-04
PHII	=	INITIAL VALUE OF ENERGY THICKNESS	=	1.0000000-04
EPSZ	=	GEOMETRY . . . AXISYMMETRIC (=1.), PLANE (=0.)	=	1.0000000+00
RBAR	=	GAS CONSTANT AT STAGNATION	=	1.1366970+02
FJ	=	CONVERSION BETWEEN THERMAL AND WORK UNITS	=	7.7820000+02
G	=	PROPORTIONALITY CONSTANT IN EQUATION -- F=M/G*A	=	3.2174000+01
SCALE	=	CONTOUR SCALE FACTOR	=	1.0000000+00

TABLE 5. C_p-T INPUT TABLE USED IN THE ORIGINAL AND MODIFIED TBL PROGRAMS

I	Specific Heat (Btu/lbm °R)	Temperature (°R)
1	6.3078549-01	7.0000000+02
2	6.6436788-01	1.6380000+03
3	7.0660707-01	2.3433153+03
4	7.2625109-01	2.5681200+03
5	7.4233390-01	2.7617400+03
6	7.6597598-01	3.0524500+03
7	7.8021657-01	3.2217000+03
8	8.1702141-01	3.6004838+03
9	9.1021608-01	4.2112448+03
10	1.1800579+00	5.1030000+03
11	1.6420093+00	6.1626920+03
12	1.6721517+00	6.2363194+03
13	1.7100503+00	6.3319866+03
14	1.7398426+00	6.4101000+03
15	1.7576111+00	6.4581300+03
16	1.7674131+00	6.4851350+03
17	1.7707793+00	6.4944977+03
18	1.7735372+00	6.5022000+03
19	1.7781478+00	6.5151568+03
20	1.7799212+00	6.6000000+03

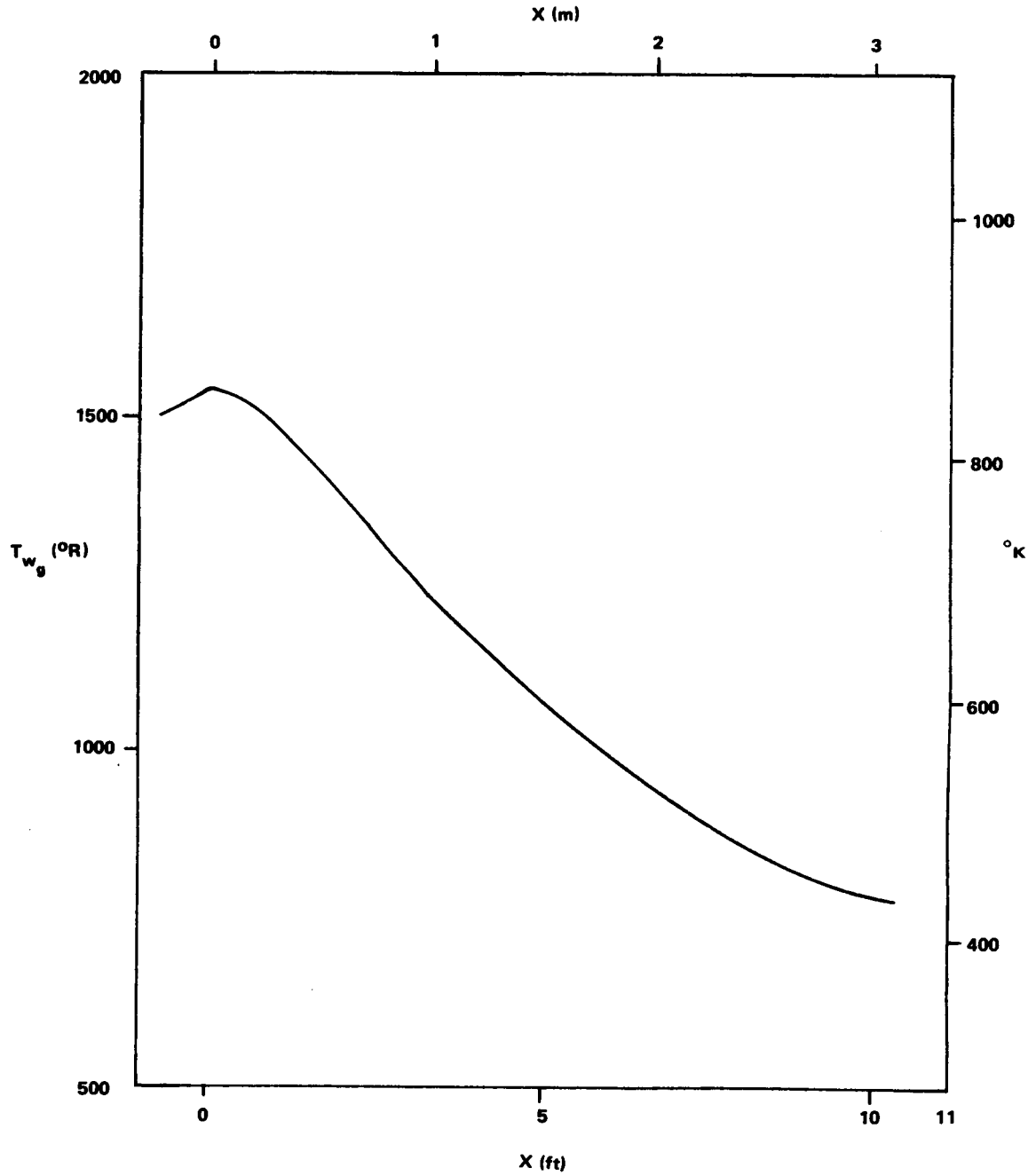

Figure 6. Nozzle wall temperature distribution (reference case).

TABLE 6. COMPARISON OF SOLUTIONS OBTAINED FROM THE MODIFIED TBL PROGRAM USING DIFFERENT WALL TEMPERATURES (REFERENCE CASE USES A VARIABLE WALL TEMPERATURE DISTRIBUTION)

	$433.3°K \leq T_{w_g} \leq 855.6°K$ $\left(780°R \leq T_{w_g} \leq 1540°R\right)$	$T_{w_g} = 888.9°K = \text{Constant}$ $\left(T_{w_g} = 1600°R = \text{Constant}\right)$
F_{vacuum}, ton (lbf)	207.658 (457 810)	206.778 (455 867)
ΔF, ton (lbf)	-1.587 (-3499)	-1.516 (-3343)
ΔI_{sp}, sec	-3.53	-3.39
$\dot{q}_{w\ max}$, kcal/cm^2 sec (Btu/in.^{2} sec)	2.802 (71.7)	2.779 (71.1)
$\dot{Q}_w$, kcal/sec (Btu/sec)	2.2574×10^4 (89 521)	2.1660×10^4 (85 895)
At nozzle exit		
δ^*, cm (ft)	1.92 (0.063)	2.13 (0.070)
δ, cm (ft)	6.00 (0.197)	6.13 (0.201)
Δ, cm (ft)	9.14 (0.300)	9.88 (0.324)
θ, cm (ft)	0.46 (0.015)	0.46 (0.015)
δ^*/θ	4.150	4.674
ϕ, cm (ft)	0.76 (0.025)	0.82 (0.027)

The boundary layer parameters, except the boundary layer velocity thickness and the momentum thickness, are higher by approximately 8 to 10 percent for the constant wall temperature profile. It should, however, be stated that the performance and heat transfer sensitivity is more pronounced if lower constant wall temperatures are considered. In Figure 4 and Figures 7 through 9, temperature thickness Δ, variation of the specific heat transfer rate $\dot{q}_w$, displacement thickness δ^*, and shape factor δ^*/θ, are plotted as a function of the axial nozzle length.

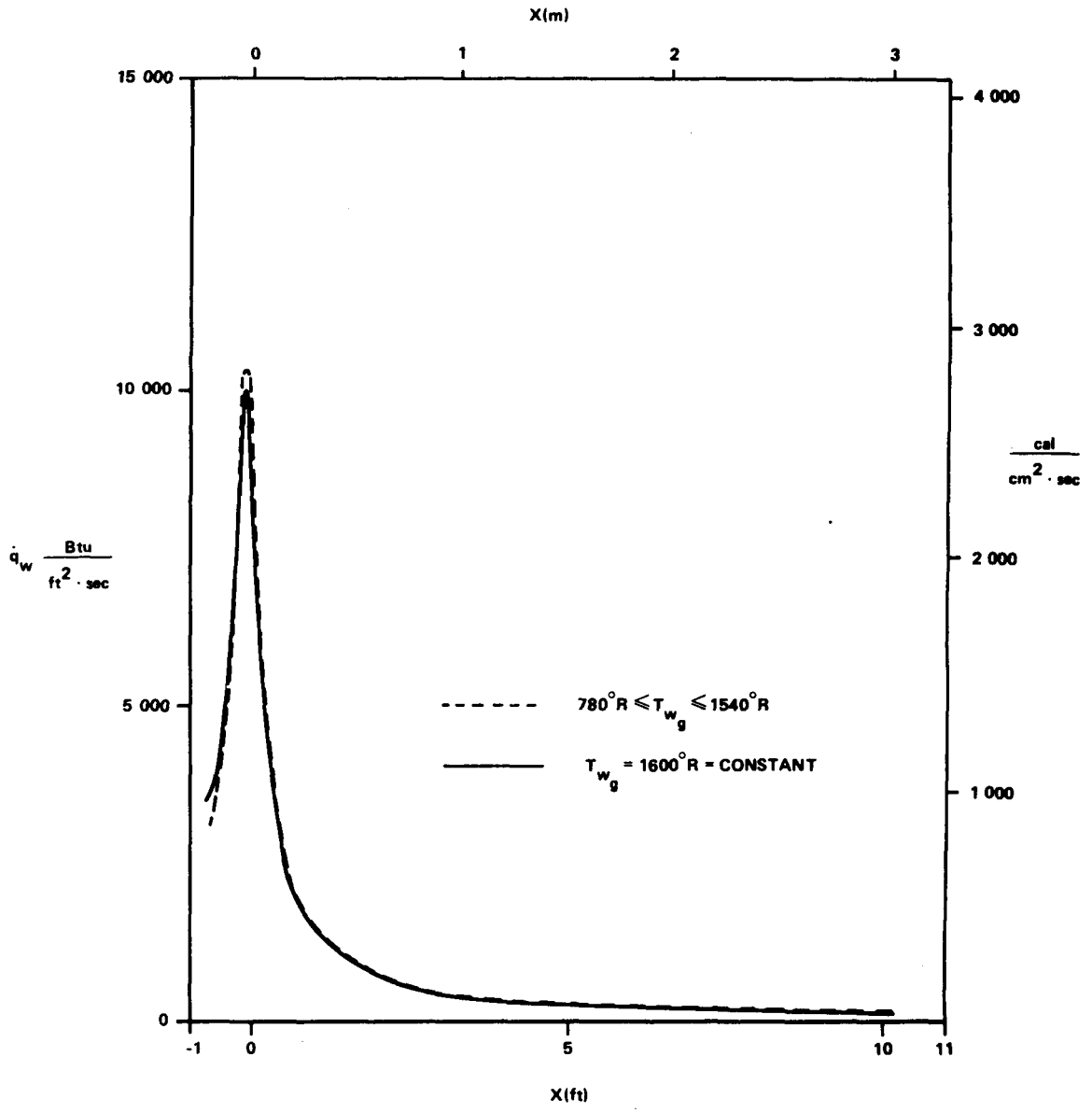

Figure 7. Specific heat transfer rate.

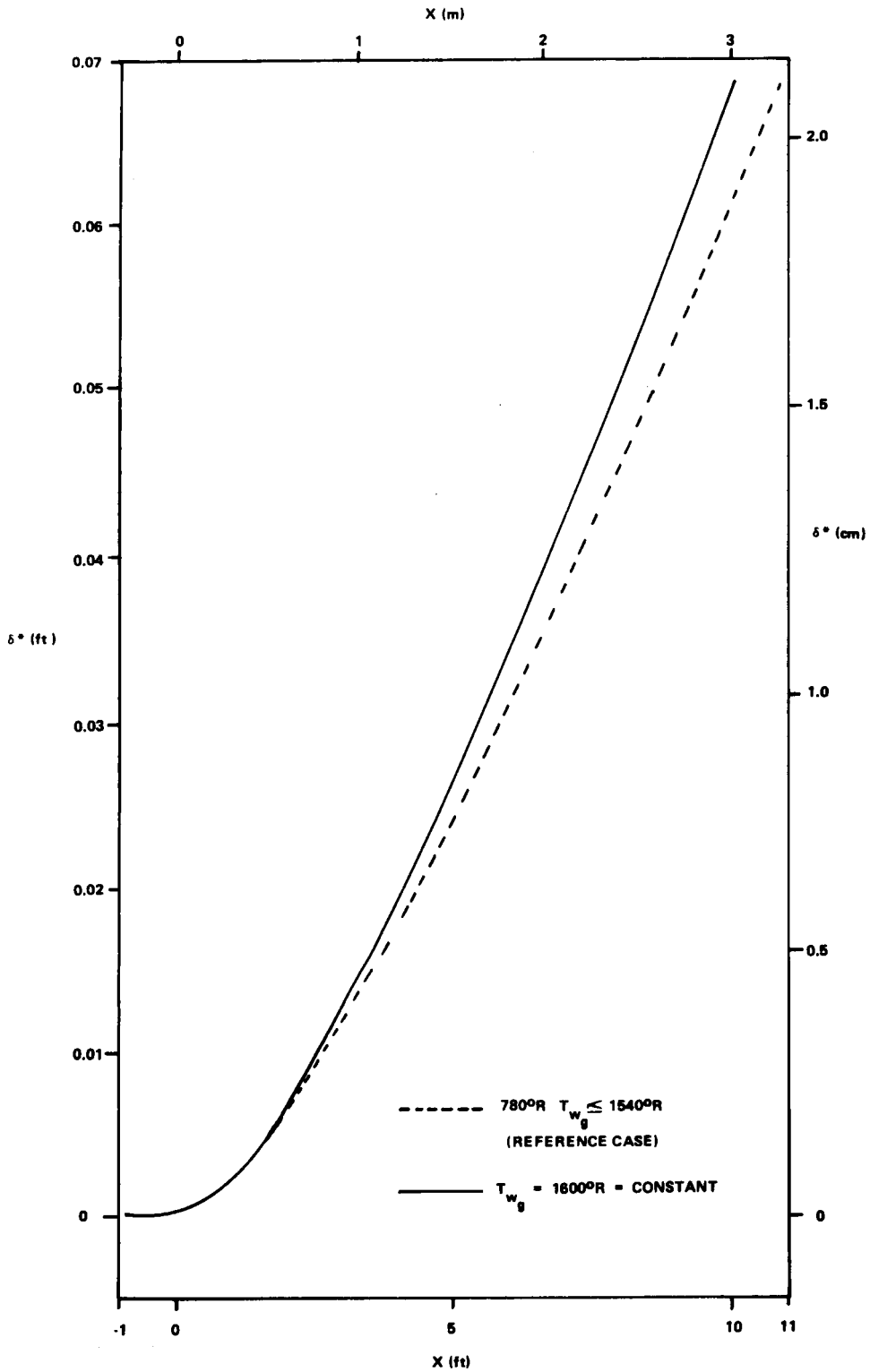

Figure 8. Effect of wall temperature on boundary layer displacement thickness.

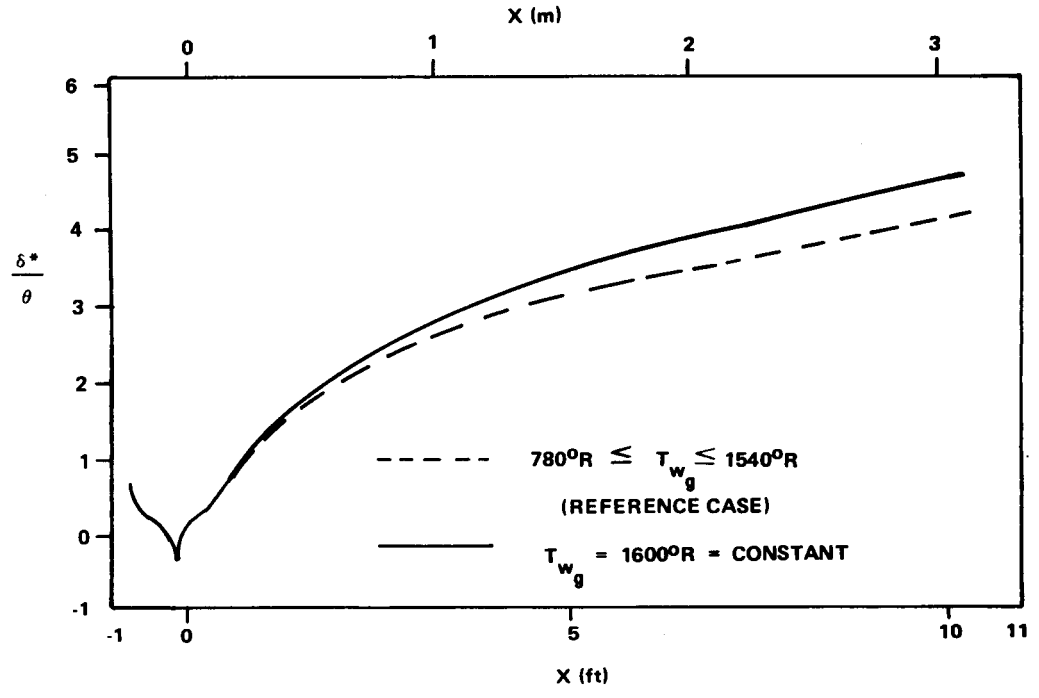

Figure 9. Effect of wall temperature on the boundary layer shape factor.

Effect of Prandtl Number

In the reference case the Prandtl number is internally calculated according to equation (7) and covers a range from 0.91 at stagnation condition to 0.80 at the nozzle exit. This equation was replaced by constant values of Prandtl number $P_r = 0.51$ and $P_r = 0.91$ during the sensitivity study. The results are presented in Table 7, and indicate that the performance degradation is hardly affected. The heat transfer rate differs significantly for the two cases of $P_r = 0.51$ and $P_r = 0.91$, whereas a negligible difference appears between the $P_r = 0.91$ and the reference case. This naturally holds true for the total heat transfer rate and indicates a 5 percent higher quantity for the $P_r = 0.51$ case compared with $P_r = 0.91$ solutions. Although the heat transfer is only slightly affected when the variable Prandtl number is replaced by $P_r = 0.91$, a considerable difference might result for high area ratio nozzles with extensive nozzle lengths. In Figure 10, the total heat transfer rate $\dot{Q}_w$ for the reference case and for $P_r = 0.51$ is shown as a function of nozzle length.

TABLE 7. COMPARISON OF SOLUTIONS OBTAINED FROM THE MODIFIED TBL PROGRAM USING DIFFERENT PRANDTL NUMBERS (REFERENCE CASE USES INTERNALLY CALCULATED PRANDTL NUMBERS)

	$P_r = 0.51$ = Constant	$P_r = 0.91$ = Constant	$0.80 \leq P_r \leq 0.91$ Variables
F_{vacuum} ton (lbf)	207.737 (457 981)	207.651 (457 793)	207.658 (457 807)
ΔF, ton (lbf)	-1.615 (-3560)	-1.586 (-3497)	-1.587 (-3499)
ΔI_{sp} (sec)	-3.59	-3.53	-3.53
$\dot{q}_{w\ max}$, kcal/cm^2 sec (Btu/in.^{2} sec)	3.096 (79.2)	2.798 (71.6)	2.802 (71.7)
$\dot{Q}_w$, kcal/sec, (Btu/sec)	2.375×10^4 (94 200)	2.2519×10^4 (89 305)	2.25474×10^4 (89 519)
At nozzle exit			
δ^*, cm (ft)	1.92 (0.063)	1.92 (0.063)	1.92 (0.063)
δ, cm (ft)	6.04 (0.198)	6.00 (0.197)	6.00 (0.197)
Δ, cm (ft)	9.48 (0.311)	9.11 (0.299)	9.14 (0.300)
θ, cm (ft)	0.46 (0.015)	0.46 (0.015)	0.46 (0.015)
δ^*/θ	4.058	4.154	4.150
ϕ, cm (ft)	0.82 (0.027)	0.76 (0.025)	0.76 (0.025)
Prandtl number	Input	Input	Internally calculated $P_r = 0.91$ at the stagnation

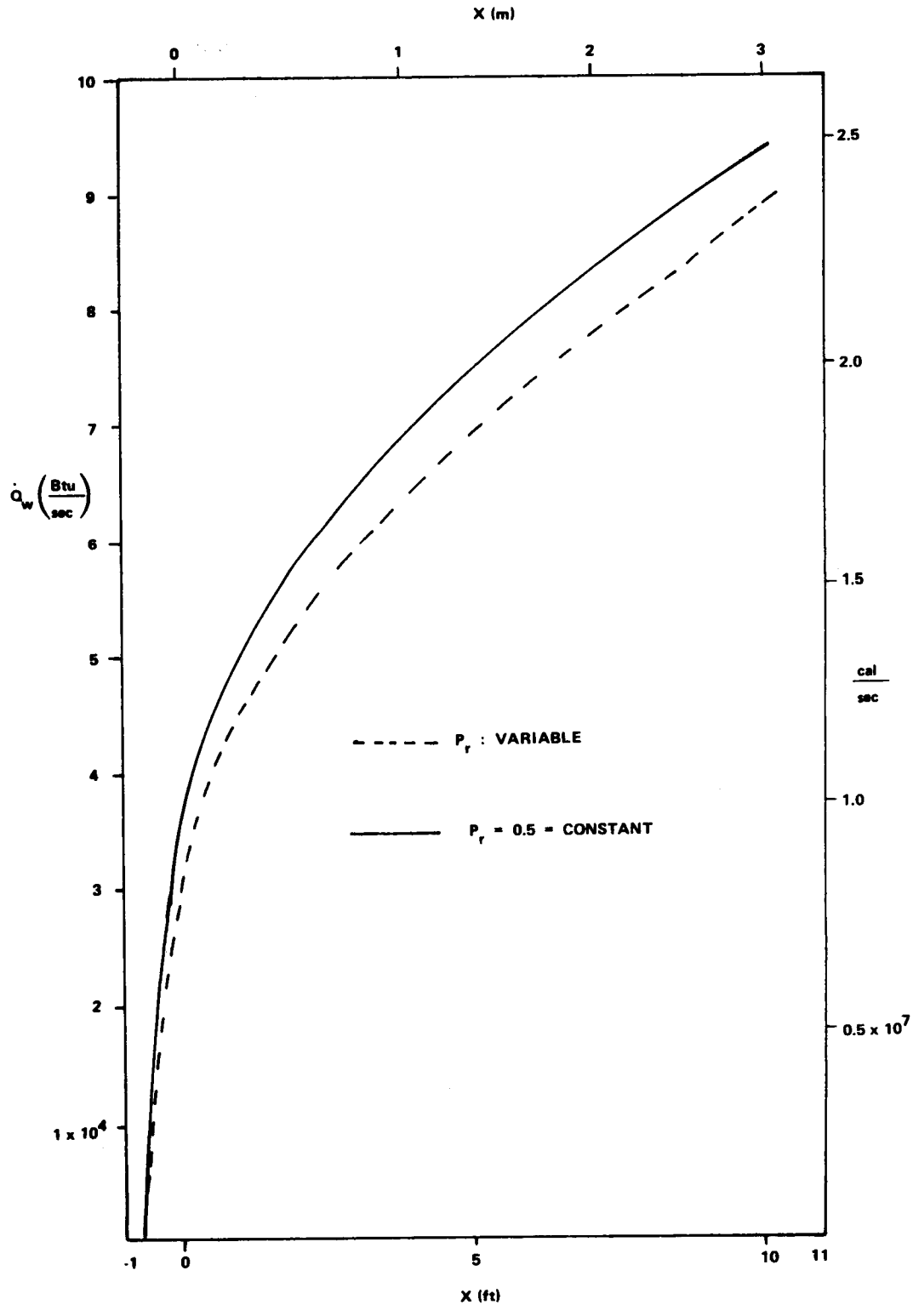

Figure 10. Effect of Prandtl number on the total heat transfer rate.

Effect of Stanton Number

The original and modified TBL programs both use the following empirical relationship to determine the Stanton number:

$$C_H = \frac{\frac{C_f\left(R_{e_\phi}\right)}{2}\left(\frac{\phi}{\theta}\right)^{\tilde{n}}}{1 - 5\left[\frac{C_f\left(R_{e_\phi}\right)}{2}\right]^{1/2}\left[1 - P_r + \ell n\left(\frac{6}{5P_r + 1}\right)\right]} \quad . \tag{24}$$

To examine the influence of Stanton number the previous equation was replaced by an equation from Reference 9 approximately representing the von Karman analogy,

$$C_H = \frac{\left[\frac{C_f\left(R_{e_\theta}\right)}{2}\right]^{1/2}}{5P_r + 5\ell n\left(5P_r + 1\right) - 14 + \left[\frac{2}{C_f\left(R_{e_\theta}\right)}\right]^{1/2}} \quad , \tag{25}$$

for this investigation only.

A total heat transfer rate increase as much as 16 percent resulted with regard to the reference case, although the performance degradation was insignificant.

Effect of Boundary Layer Velocity Profile

The velocity profile across the boundary layer is commonly expressed by a power law,

$$\frac{u}{U_\infty} = \left(\frac{y}{\delta}\right)^{1/n} \quad , \tag{26}$$

The recommended value for n in the exponent is $n = 7$. This number has been used for the reference case although n is a program variable. Reference 5 concludes that n changes with the Reynolds number and pressure gradient, and varies between $n = 5$ and $n = 9$ for a Mach number range from $M = 3.85$ to $M = 4.8$. It is shown in Reference 10 that $n = 8$ and 5 for Mach numbers $M = 5$ and 8, respectively. In studying the velocity profile effects on the boundary layer solutions, a value of $n = 5$ was selected in the power law. The results for the reference case and using $n = 5$ are presented in Table 8. A specific impulse loss increase of approximately 8 percent occurs when the exponent factor n is changed from $n = 7$ to $n = 5$, whereas a slight decrease in the total heat transfer rate is experienced. Figure 5 and Figures 11 through 13 show the velocity thickness δ, displacement thickness δ^*, momentum thickness θ, and shape factor δ^*/θ as a function of the nozzle length for the reference case and the one using $n = 5$. These parameters are affected considerably by the velocity power law, especially the velocity thickness δ, and the effect increases with nozzle length.

RESULTS OF THE PARAMETER STUDY AFFECTING PERFORMANCE AND HEAT TRANSFER

For convenience the energy thickness ϕ and the Reynolds number based upon the momentum thickness R_{e_θ} as a function of the nozzle length are provided for the reference case in Figures 14 and 15. Variation of the Reynolds number in the throat section is very large because of the influences of density, velocity, and momentum thickness.

In Figure 16 the performance degradation in terms of specific impulse is presented as a function of nozzle length. Results obtained with the original and modified TBL programs as well as changes caused by the variation of the wall temperature and velocity profile with respect to the modified TBL version are exhibited. The effects of the Prandtl and Stanton numbers are not specifically shown, since the curves fall almost on top of the reference case. (See Table 7 and the section entitled "Effect of Stanton Number".)

It is evident that the largest variation in the performance degradation occurs when the free-stream parameters calculated internally by a perfect gas analogy are replaced by more accurate input tables. The wall temperature and to a greater extent the velocity profile are significant parameters and must be accurately determined for a performance degradation analysis.

TABLE 8. COMPARISON OF SOLUTIONS OBTAINED FROM THE MODIFIED TBL PROGRAM USING DIFFERENT FACTORS n IN THE VELOCITY PROFILE EXPONENT (n = 7, REFERENCE CASE)

	n = 7	n = 5
F_{vacuum}, ton (lbf)	207.658 (457 810)	208.643 (459 980)
ΔF, ton (lbf)	-1.587 (-3499)	-1.720 (-3792)
ΔI_{sp}, sec	-3.53	-3.80
$\dot{q}_{w\ max}$, kcal/cm^2 sec (Btu/in.^{2} sec)	2.802 (71.7)	2.802 (71.7)
Q_w, kcal/sec (Btu/sec)	2.2574×10^4 (89 521)	2.2490×10^4 (89 190)
At nozzle exit		
δ^*, cm (ft)	1.92 (0.063)	1.71 (0.056)
δ, cm (ft)	6.00 (0.197)	5.09 (0.167)
Δ, cm (ft)	9.14 (0.300)	7.32 (0.240)
θ, cm (ft)	0.46 (0.015)	0.49 (0.016)
δ^*/θ	4.150	3.488
ϕ, cm (ft)	0.76 (0.025)	0.76 (0.025)
$\frac{u}{U_\infty}$	$\frac{u}{U_\infty} = \left(\frac{y}{\delta}\right)^{1/7}$	$\frac{u}{U_\infty} = \left(\frac{y}{\delta}\right)^{1/5}$

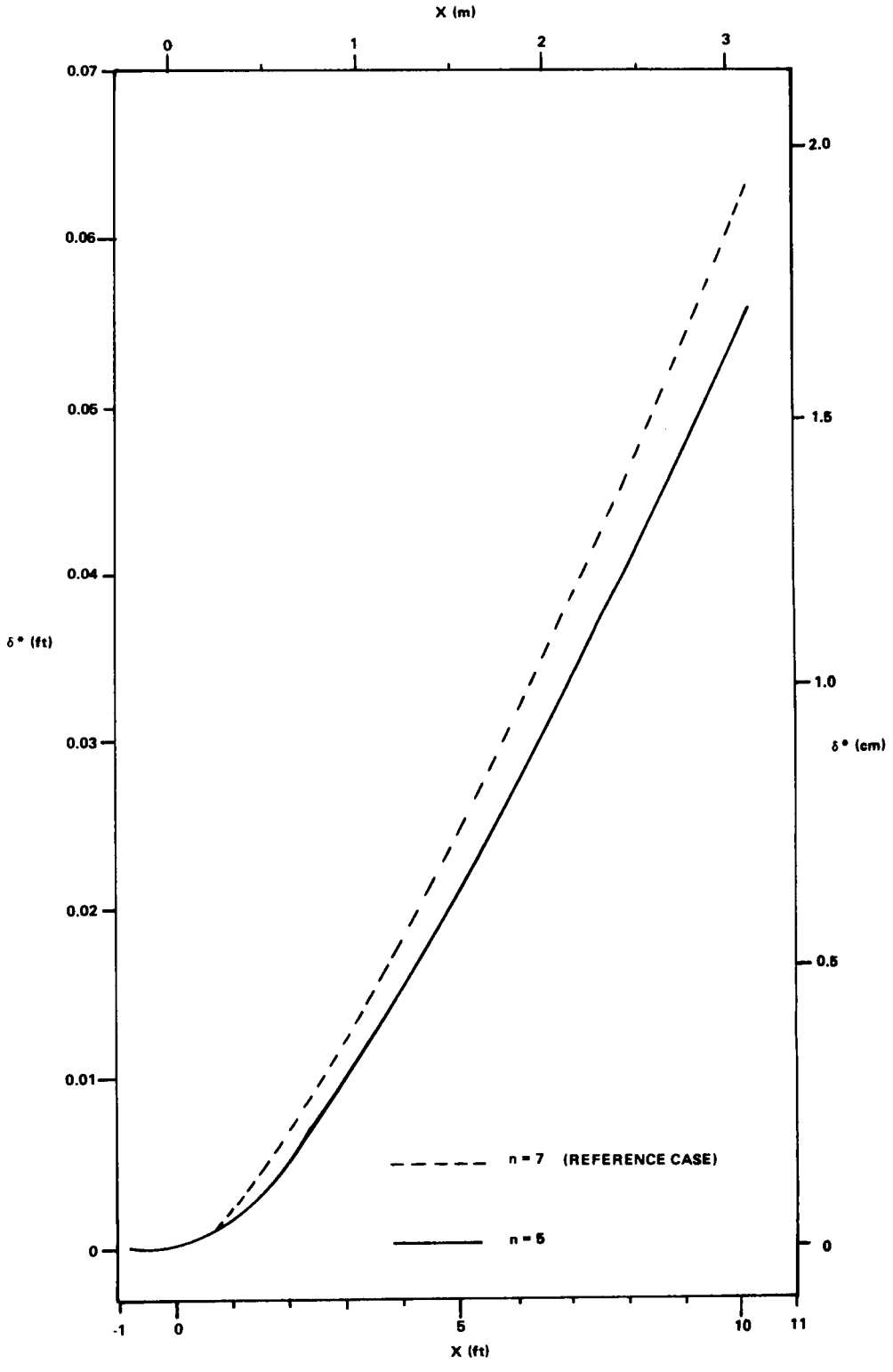

Figure 11. Effect of velocity profile power law on the boundary layer displacement thickness.

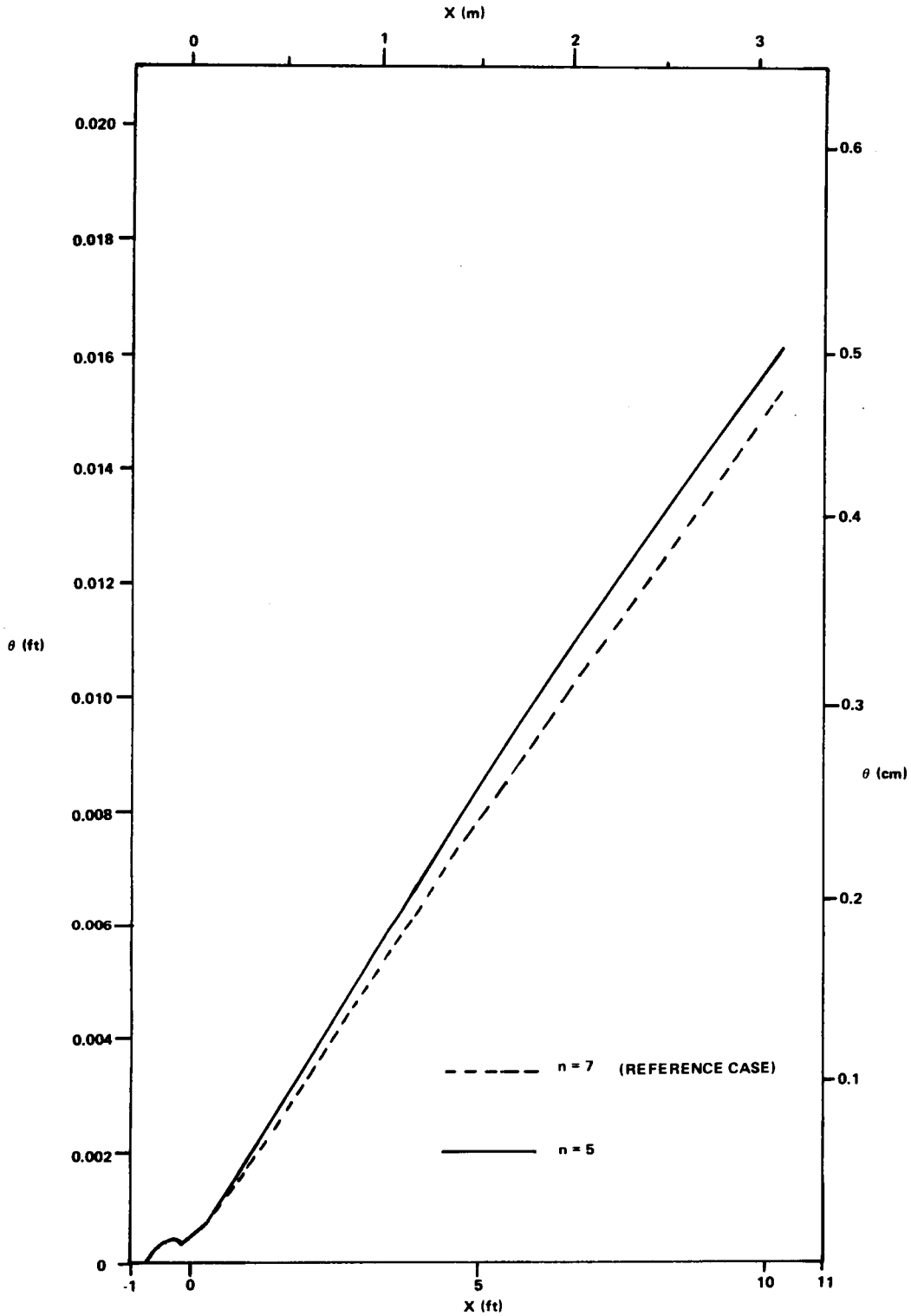

Figure 12. Effect of velocity profile power law on the momentum thickness.

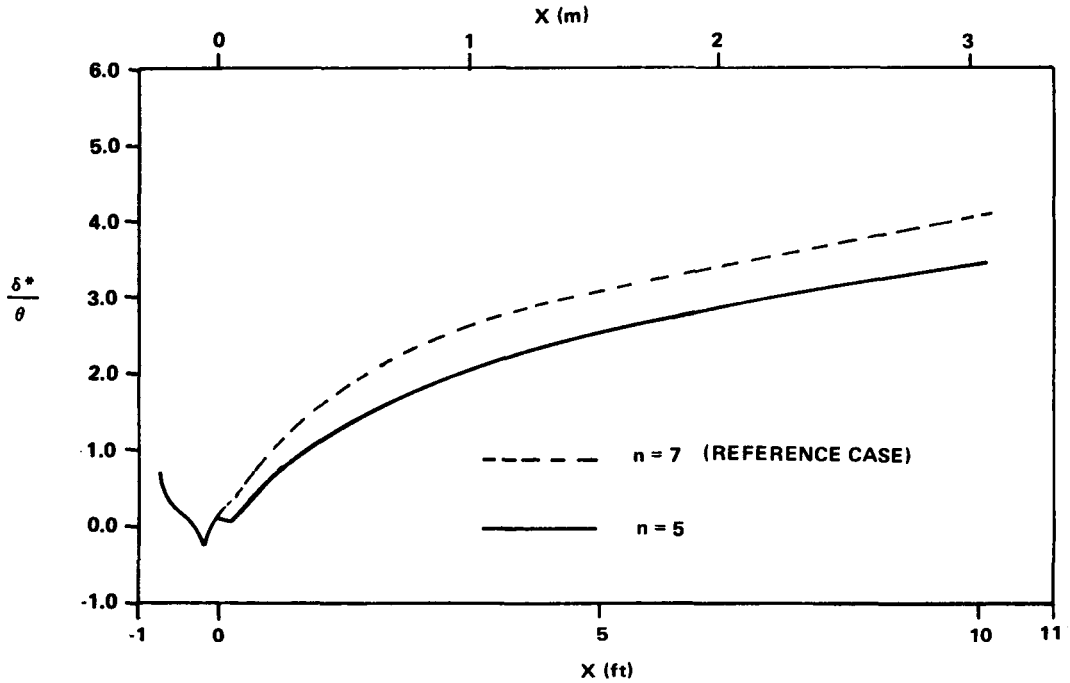

Figure 13. Effect of velocity profile power law on the boundary layer shape factor.

As to the heat transfer, a sizable difference has been experienced when the original TBL solutions are compared with the modified TBL results. The Prandtl and Stanton numbers affect the heat transfer significantly, whereas the velocity profile produces only a small variation. The selected constant wall temperature indicated only a minor effect on the heat transfer. However, lower wall temperatures might have a much larger influence. Table 9 represents a quantitative estimate of the influence of the parameters investigated on the performance, heat transfer, and boundary layer parameters.

CONCLUSIONS

The original TBL program has been modified to accept boundary layer edge conditions from an external source. In addition, several equations within the program were modified, and new ones were introduced. A former Space Shuttle engine design was used to investigate how the boundary layer solutions were changed by the modifications. Comparison of the results indicated drastic differences in the performance degradation, heat transfer, and the

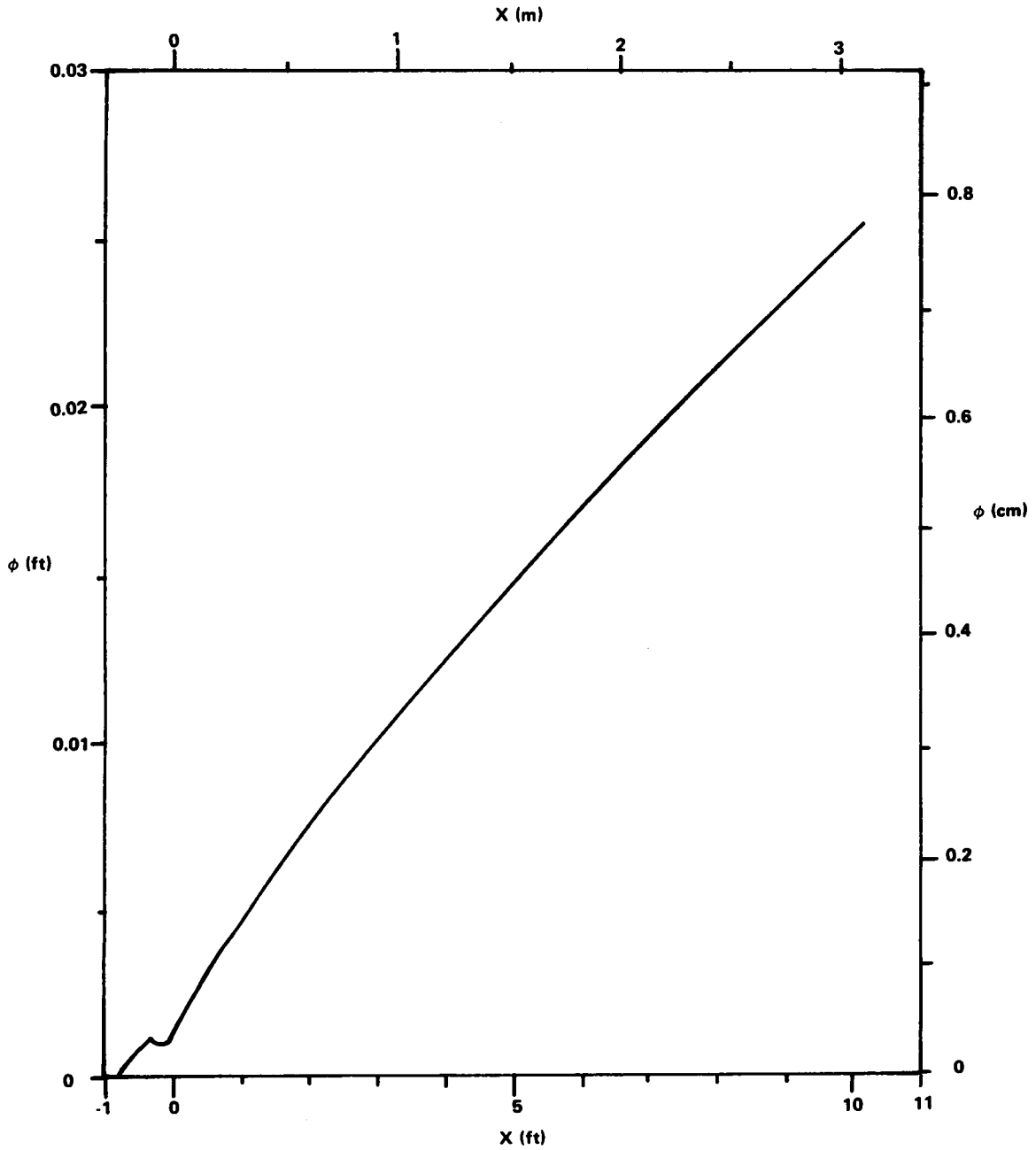

Figure 14. Energy thickness as a function of nozzle length (reference case).

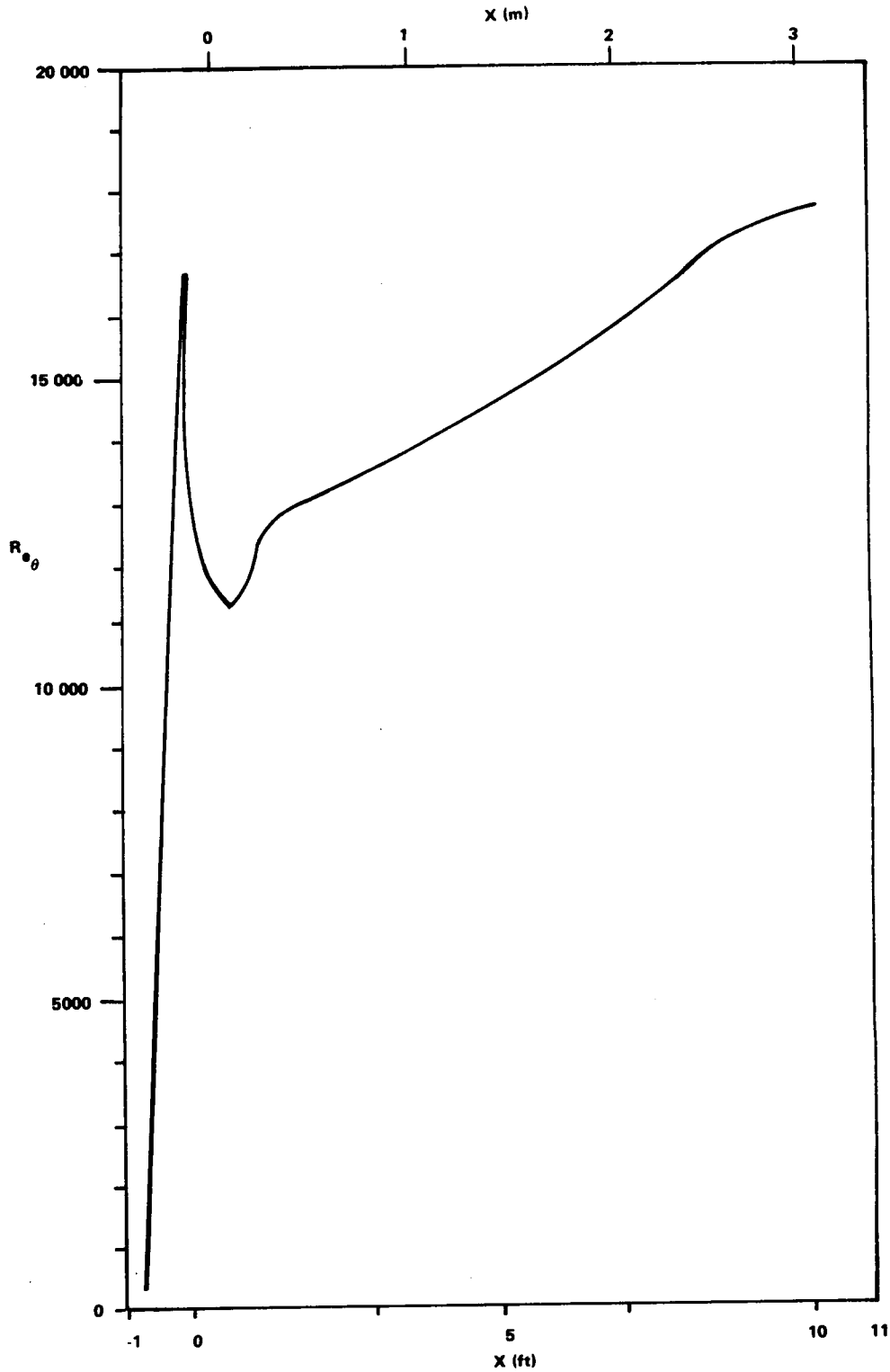

Figure 15. Reynolds number as a function of nozzle length (reference case).

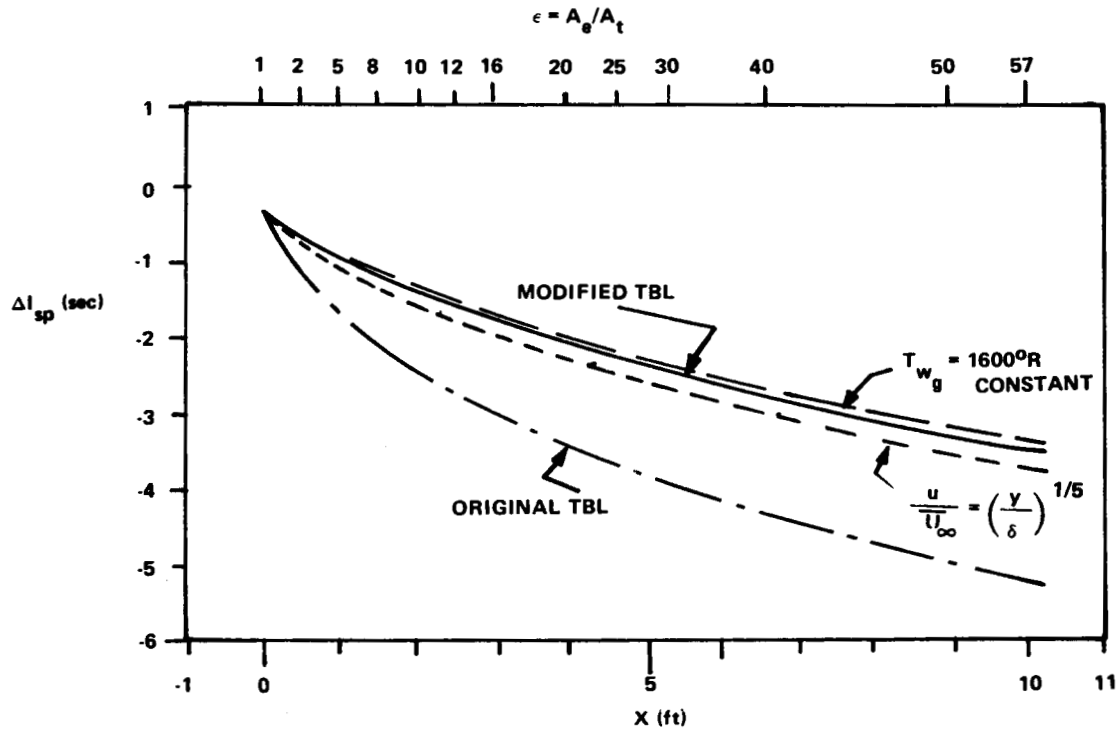

Figure 16. Specific impulse loss caused by boundary layer effects.

magnitude of boundary layer parameters. During a parametric study investigating the effect of significant parameters on heat transfer and performance, results from the modified TBL program were used as a reference. A comparison of the results indicated the strong influence of the velocity profile, and to a minor degree the wall temperature, on performance. The heat transfer rate was primarily influenced by the Prandtl and Stanton numbers. The influence of the wall temperature depends on the magnitude of the temperature.

TABLE 9. QUANTITATIVE ESTIMATE OF THE INFLUENCE OF INVESTIGATED PARAMETERS ON PERFORMANCE, HEAT TRANSFER, AND BOUNDARY LAYER PARAMETERS

	P_r	C_H	C_f	$\frac{u}{U_\infty} = \left(\frac{y}{\delta}\right)^{1/n}$	T_{w_g}	Solution Differences Between Original TBL and Modified TBL
F_{vacuum}	1	2	2	2	1	4
ΔF	1	2	4	2	2	5
ΔI_{sp}	1	3	4	2	2	5
$\dot{q}_{w\ max}$	2	5	4	1	1	4
$\dot{Q}_w$	2	5	4	2	2	3
δ^*	1	3	4	3	2	5
δ	1	3	4	4	1	4
Δ	1	3	3	3	2	2
θ	1	3	4	2	1	3
ϕ	1	2	2	1	2	3

Notes: Influence; 1 — negligible, 2 — slight, 3 — considerable, 4 — large, and 5 — extreme.

APPENDIX A
DERIVATION OF PRANDTL NUMBER

Let us denote the specific heat at constant volume as C_v (cal/gr °C), then the specific heat for one molecule with mass, m, is mC_v (cal/°C). This is the increase in kinetic energy of a molecule with a temperature rise of 1°C.

When a temperature gradient, dT/dx, exists in a gas, the temperature difference of two molecules that are separated by a distance of $2\bar{\ell}$, is equal to $2\bar{\ell}$ (dT/dx). Therefore, the energy difference between these molecules is:

$$mC_v \times 2\bar{\ell} \frac{dT}{dx} \quad . \tag{A-1}$$

Consider the mean-free-path length which is the average distance a molecule may travel before it collides with another molecule. The above two molecules exchange their energies by such a collision. Averaging the total molecules moving at random, we can assume that they move an amount of one-sixth in each direction of the Cartesian coordinates x, y, and z. By assuming there are N molecules per 1 cm^3 of a gas and their mean molecular velocity is $\bar{v}$ (cm/sec), the number of molecules moving in one direction across the area of 1 cm^2 in 1 second is $N\bar{v}/6$. These transfer energies, as stated above, and their total heat transfer rate (cal/cm^2 sec) is:

$$\lambda \frac{dT}{dx} \quad , \tag{A-2}$$

which is called the Fourier law. The thermal conductivity is λ (cal/cm sec °C) and has a certain value depending upon the substance; therefore, we obtain:

$$\lambda \frac{dT}{dx} = mC_v \times 2\bar{\ell} \frac{dT}{dx} \times \frac{N\bar{v}}{6} \quad , \tag{A-3}$$

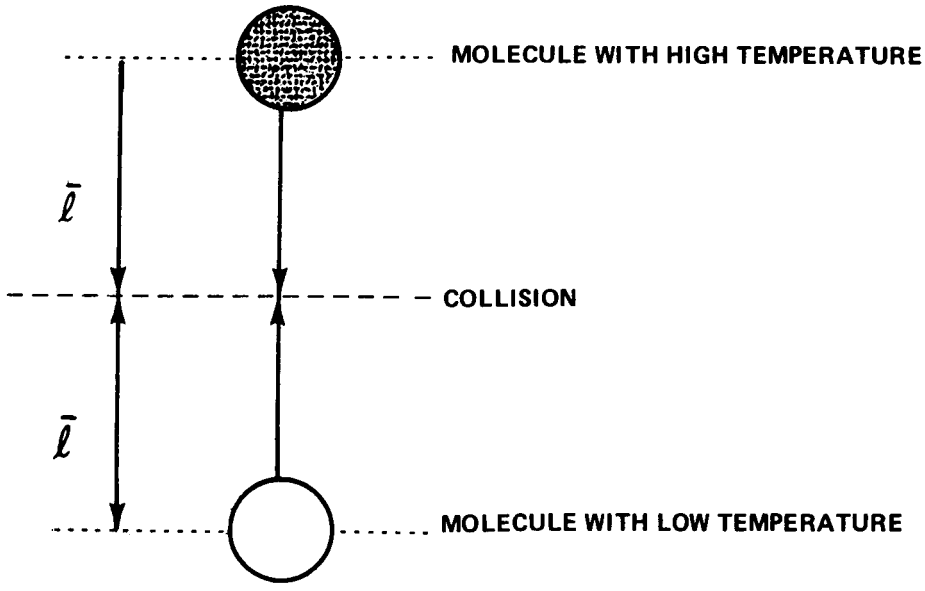

so that

$$\lambda = \frac{1}{3} Nm\bar{v}\bar{\ell} C_v = \frac{1}{3} \rho \bar{v} \bar{\ell} C_v \qquad (A-4)$$

where $\rho = Nm$ is the density of the gas.

Another relation for the thermal conductivity is derived in Appendix B,

$$\lambda = \frac{1}{3} \frac{9\gamma - 5}{4\gamma} \rho \bar{v} \bar{\ell} C_p \quad , \qquad (A-5)$$

where γ is the ratio of the specific heat at constant pressure to that at constant volume, $\gamma = C_p/C_v$.

The viscosity of a gas is also caused by molecular collisions. By considering the momentum exchange between colliding molecules in a gas along with velocity gradients, the viscosity coefficient μ (gr/cm sec) can be easily derived as in the case of equation (A-4),

$$\mu = \frac{1}{3} \rho \bar{v} \bar{\ell} \quad . \qquad (A-6)$$

By dividing both terms of equations (A-5) and (A-6) respectively, we obtain:

$$\frac{\mu C_p}{\lambda} = \frac{4\gamma}{9\gamma - 5} \quad . \tag{A-7}$$

The left side of equation (A-7) is the definition of the Prandtl number, P_r. Rearranging equation (A-7) results in

$$P_r = \frac{C_p}{\frac{9}{4} C_p - \frac{5}{4} C_v}$$

$$= \frac{C_p}{C_p + \frac{5}{4} C_p - \frac{5}{4} C_v} \quad .$$

Using the ideal gas relationship,

$$C_p - C_v = \frac{\mathcal{R}}{\mathfrak{M}} \quad ,$$

finally yields

$$P_r = \frac{C_p}{C_p + \frac{5}{4} \frac{\mathcal{R}}{\mathfrak{M}}} \quad . \tag{A-8}$$

APPENDIX B
DERIVATION OF THERMAL CONDUCTIVITY

The internal energy of a molecule is composed of a transverse movement, rotation, and internal vibration. Therefore, the specific heat, C_v, is composed of the components C_{vt}, C_{vr}, and C_{vo}:

$$C_v = C_{vt} + C_{vr} + C_{vo} \quad . \tag{B-1}$$

Since the mean velocity of molecules is higher for those with higher temperature, the energy transfer by the transverse movement is large. According to Chapman[1] λ is as much as 2.5 times as great when molecules have only the degree of freedom of transverse movement instead of rotation or vibration only. Eucken[2] considered that influences of the rotation and internal vibration on the energy transfer are small even when both exist at the same time; then, equation (A-4) is

$$\lambda = \frac{1}{3} \rho \bar{v} \bar{\ell} \ (2.5\, C_{vt} + C_{vr} + C_{vo}) \quad . \tag{B-2}$$

Substituting the following relations into equation (B-2), we obtain equation (A-5). Equation (B-1) becomes after rearrangement

$$C_{vr} + C_{vo} = C_v - C_{vt} \quad . \tag{B-3}$$

Using the gas dynamics relation,

$$C_{vt} = \frac{3}{2} \frac{\mathcal{R}}{\mathfrak{M}} \quad ; \tag{B-4}$$

---

1. Chapman, S.: Phil. Trans., vol. A211, 1912, p. 459.
2. Eucken, A.: Forsch. Gebiete Ingenieurw., vol. 11, no. 6, 1940.

and the ideal gas formulation,

$$C_p - C_v = \frac{\mathcal{R}}{\mathfrak{M}} \quad . \tag{B-5}$$

In equation (B-2), the following result for the thermal conductivity is obtained:

$$\lambda = \frac{1}{3} \rho \bar{v} \bar{\ell} \left(\frac{9}{4} C_p - \frac{5}{4} C_v \right)$$

$$= \frac{1}{3} \frac{9\gamma - 5}{4\gamma} \rho \bar{v} \bar{\ell} C_p . \tag{B-6}$$

APPENDIX C
SKIN FRICTION COEFFICIENT

The skin friction coefficient calculation in the original TBL program is based upon the following computation loop [11]. Initially an adiabatic skin friction coefficient C_{f_a} is assumed. Then a corresponding skin friction coefficient for low speed flow $\bar{C}_f$ is calculated using Cole's relationship,

$$\bar{C}_f = \frac{\rho \mu_s}{\rho_{aw} \mu_{aw}} \cdot C_{f_a} \tag{C-1}$$

where the subscript aw refers to adiabatic wall conditions, ρ is the free stream density, and μ_s represents the dynamic viscosity of the laminar sublayer. The dynamic sublayer viscosity μ_s is obtained using Cole's temperature relationship.

$$\frac{T_s}{T_{aw}} = 1 + 17.2 \left(\frac{T_0}{T_{aw}} - 1 \right) \left(\frac{\bar{C}_f}{2} \right)^{1/2} - 305 \left(\frac{T_0}{T_{aw}} - \frac{T}{T_{aw}} \right) \frac{\bar{C}_f}{2} , \tag{C-2}$$

in connection with

$$\frac{\mu_s}{\mu_{aw}} = \left(\frac{T}{T_{aw}} \right)^m , \tag{C-3}$$

where the exponent n denotes the temperature dependence of viscosity.

The following expression is then calculated according to Cole:

$$\bar{C}_f \cdot \bar{R}_{e_{\bar{\theta}}} = \frac{\rho \mu}{\rho_{aw} \mu_{aw}} \cdot C_{f_a} \cdot R_{e_\theta} . \tag{C-4}$$

This equation is similar to the previous one except that the free stream dynamic viscosity μ and the Reynolds number based upon the momentum thickness,

$$R_{e_\theta} = \frac{\rho U \theta}{\mu} \quad , \tag{C-5}$$

are used. Now another low speed flow skin friction coefficient C_f can be determined using

$$\bar{C}_f = \frac{0.009896}{\left(\bar{C}_f \bar{R}_{e_{\bar{\theta}}}\right)^{0.562}} \tag{C-6}$$

for a range of $\bar{C}_f \bar{R}_{e_\theta} = 1$ to 2.51 , a tabular relationship based on test data over the range of $\bar{C}_f \bar{R}_{e_{\bar{\theta}}} = 2.51$ to 64.8 , and

$$\left(\frac{2}{\bar{C}_f}\right)^{1/2} = 2.44 \ell n \left[\frac{\bar{C}_f \bar{R}_{e_{\bar{\theta}}}}{\bar{C}_f \left(3.781 - \frac{25.104}{\left(\frac{2}{\bar{C}_f}\right)^{1/2}}\right)} \right] + 7.68 \tag{C-7}$$

for values of $\bar{C}_f \bar{R}_{e_{\bar{\theta}}} > 64.8$.

The resulting skin friction coefficient $\bar{C}_f$ is then compared to the coefficient assumed initially. If both values of $\bar{C}_f$ fall within a small tolerance, C_{f_a} is satisfactorily determined, otherwise the calculation must be repeated with an improved C_{f_a} assumption.

Application of the TBL program to a former Space Shuttle engine design, which was selected as a reference case in this document, observed that a plot representing the adiabatic skin friction coefficient as a function of the Reynolds number, showed multiple solutions for a constant Reynolds number for $R_{e_\theta} > 10^4$ (Fig. 1). Test data, however, indicate that such condictions do not exist. Therefore the previously described solution method for the skin friction coefficient was replaced by the following straightforward method. At first the Reynolds number at a specific location is calculated by

$$R_{e_\theta} = \frac{\rho U \theta}{\mu} \quad . \tag{C-8}$$

Then the skin friction coefficient is directly determined from the relation,

$$C_f = \frac{K}{\left(R_{e_\theta}\right)^{0.25}} \quad . \tag{C-9}$$

According to experiments by D. Brott [5] the constant $K = 0.018$ for Mach numbers $M > 1$ with pressure gradients in the flow. In the modified TBL program a constant $K = 0.025$ was used instead representing more closely the Blasius relationship. From Figure 1 it is evident that solutions for the skin friction coefficient very closely compare with the original TBL concept; however, multiple solutions for Reynolds numbers $R_{e_\theta} > 10^4$ are avoided.

REFERENCES

1. TBL, Turbulent Boundary Layer Nozzle Analysis Computer Program. Developed by Pratt and Whitney Aircraft, ICRPG, 1969.

2. Omori, S.; Krebsbach, A; and Gross, K. W.: Supplement to the ICRPG Turbulent Boundary Layer Nozzle Analysis Computer Program. NASA TM X-64663, 1972.

3. ODK, One-Dimensional Kinetic Nozzle Analysis Computer Program. Developed by NASA-Lewis Research Center, ICRPG, 1970.

4. TDK, Two-Dimensional Kinetic Nozzle Analysis Computer Program Developed by Dynamic Science, ICRPG, 1970.

5. Brott, D. L.; Yanta, W. J.; Voisinet, R. L.; and Lee, R. E.: An Experimental Investigation of the Compressible Turbulent Boundary Layer with a Favorable Pressure Gradient. AIAA J., vol. 8, 1970, pp. 1270-1274.

6. Gross, K. W.: Calculation of Rocket Performance Parameters Based on the Equilibrium Composition of the Combustion Products. NASA TM X-53334, 1965.

7. Space Shuttle Main Engine — Preliminary Design Review. BC 70-105, Rocketdyne, North American Rockwell, Combustion Devices and Stability Splinter Meeting, December 1970.

8. Space Shuttle Main Engine Preliminary Design Review (Combustion Components and Stability). Aerojet Liquid Rocket Company, December 1970.

9. Back, L. H.; Massier, P. F.; and Gier, H. L.: Convective Heat Transfer in a Convergent-Divergent Nozzle (Revision No. 1). JPL-TR-32-415, Jet Propulsion Laboratory, California Institute of Technology, February 1965.

10. Spence, D. A.: Velocity and Enthalpy Distribution in the Compressible Turbulent Boundary Layer on a Flat Plate. J. Fluid Mech., vol. 8, 1960, pp. 368-387.

11. Elliott, D. G.; Bartz, D. R.; and Silver, S.: Calculation of Turbulent Boundary-Layer Growth and Heat Transfer in Axi-Symmetric Nozzles. NASA TR-32-387, 1963.

APPROVAL

BOUNDARY LAYER LOSS SENSITIVITY STUDY USING A MODIFIED ICRPG TURBULENT BOUNDARY LAYER COMPUTER PROGRAM

By Satoaki Omori, Alfred Krebsbach, and Klaus W. Gross

The information in this report has been reviewed for security classification. Review of any information concerning Department of Defense or Atomic Energy Commission programs has been made by the MSFC Security Classification Officer. This report, in its entirety, has been determined to be unclassified.

This document has also been reviewed and approved for technical accuracy.

Karl L. Heimburg

KARL L. HEIMBURG
Director, Astronautics Laboratory

☆U. S. GOVERNMENT PRINTING OFFICE: 1972—745-885/4097 Region 4

DISTRIBUTION

INTERNAL

DIR

DEP-T

AD-S
Dr. G. C. Bucher (2)

A&TS-PAT
Mr. L. D. Wofford, Jr.

PM-PR-M

A&TS-MS-H

A&TS-MS-IP (2)

A&TS-MS-IL (8)

A&TS-TU (6)

S&E-ASTN-DIR
Mr. K. L. Heimburg (2)
Dr. R. R. Head

S&E-ASTN-P
Mr. H. Paul

S&E-ASTN-PPB
Mr. K. W. Gross (50)
Dr. S. Omori (10), Postdoctoral Research Associate of National Research Council
Mr. A. Krebsbach (20)

EXTERNAL

Scientific and Technical Information Facility (25)
P. O. Box 33
College Park, Maryland 20740
Attn: NASA Representative (S-AK/RKT)

Chemical Propulsion Information Agency (5)
Applied Physics Laboratory
8621 Georgia Avenue
Silver Spring, Maryland 20910
Attn: Mr. Tom Reedy

National Research Council, National Academy of Sciences (2)
2101 Constitution Avenue
Washington, D. C. 20418
Attn: Dr. T. H. Curry